DIFFERENTIATION OF THYROID CELLS TO PARATHYROID CELLS IN COCULTURE ENVIRONMENT

by
Gülçin Delal Nozhatzadeh

Submitted to Graduate School of Natural and Applied Sciences
in Partial Fulfillment of the Requirements
for the Degree of Master of Science in
Biotechnology

Yeditepe University
2021

DIFFERENTIATION OF THYROID CELLS TO PARATHYROID CELLS IN COCULTURE ENVIRONMENT

APPROVED BY:

Prof. Dr. Gamze TORUN KÖSE ……
(Thesis Supervisor)
(Yeditepe University)

Prof. Dr. Mustafa Erhan AYŞAN ……
(Yeditepe University)

Assoc. Prof. Dr. Seda KIZILEL ……
(Koç University)

DATE OF APPROVAL: …./…./2021

I hereby declare that this thesis is my own work and that all information in this thesis has been obtained and presented in accordance with academic rules and ethical conduct. I have fully cited and referenced all material and results as required by these rules and conduct, and this thesis study does not contain any plagiarism. If any material used in the thesis requires copyright, the necessary permissions have been obtained. No material from this thesis has been used for the award of another degree.

I accept all kinds of legal liability that may arise in case contrary to these situations.

Name, Last name Gülçin Delal, Nozhatzadeh

Signature …..……..……..

ACKNOWLEDGEMENTS

First and foremost, I would like to express my sincere gratitude and deepest appreciation to my thesis advisor Prof. Dr. Gamze TORUN KÖSE for providing me chance to involve in this study. I also thank her for her endless guidance and scientific support. It was an honor to be accepted to conduct my graduation project under her supervision.

I am also immensely grateful to Prof. Dr. Erhan AYŞAN for helping me in this study with his invaluable expertise in parathyroid studies. I couldn't be able to complete this thesis without his persistent help, worthwhile comments and suggestions which challenged me to broaden my perspective.

I would also like to thank Dr. Özge KARABIYIK ACAR for her constant assistance and guidance. I am grateful to experience her curiosity and enthusiasm for science. I also want to thank my fellow lab mate Ahmed Alperen TUNCER for not only working together but also encouraging me throughout the whole thesis.

I must express my very profound gratitude to my colleagues Batoul YOUSEF, Didem AKSU, Kardelen TÜFEKÇİ, İrem BÜYÜK and Sezer AKGÖL for their academic support and always staying by my side. Special thanks go to my lovely friends Aylin BALCIOĞLU, Barış ERDİNÇER, Begüm ÜNAL, Bilge KABACAOĞLU, Ecem NURÇİN and Elif EMİR for their generous love. I can't imagine how I could make it until the end without your mental and moral support.

Above all, I would like to thank my dearest parents Gönül and Karim NOZHATZADEH for their confidence in all choices I made throughout my life. Their never-ending patience, support and unlimited love make me the person who I am. Feeling their encouragement in all aspects makes life worth living.

ABSTRACT

DIFFERENTIATION OF THYROID CELLS TO PARATHYROID CELLS IN COCULTURE ENVIRONMENT

Parathyroid (Pt) is the only organ responsible for the secretion and release of parathormone (PTH), which regulates calcium and phosphorus homeostasis. Many essential physiological reactions in the body depend on the maintenance of this homeostasis. Imbalance in serum calcium causes many metabolic problems. Hypoparathyroidism is a condition characterized by low serum PTH, low calcium and high phosphate levels. The classical treatment of hypoparathyroidism consists of calcium and vitamin D supplementation. Recombinant human PTH preparations can also be used, but they are mostly not preferred because of their high cost. The most effective and permanent treatment option is parathyroid allo-transplantation (Pt allo-tx). The biggest problem in Pt allo-tx is finding a suitable donor and immune rejection. Various tissue engineering studies are carried out to overcome these problems, but still the problem has not been solved completely. In this study, it was aimed to create Pt organoid from stem cells of thyroid tissue, which has the same embryological origin as the parathyroid, in a coculture (COC) environment. Activin A and sonic hedgehog (Shh) were used as differentiation factors. After 14 days of incubation, differentiation was evaluated by gene expression profile analysis, biochemical PTH secretion measurement, and immunohistochemical (IHC) assessment. The actual measured PTH release values of the formed COC organoids were higher than the expected PTH release values, and statistically significant increases in PTH release were observed between day 2 and day 14. By qPCR analysis, Pt specific PTH and CaSR gene expressions of the COC organoids were examined and increase in PTH (between 4.0 and 8.8 fold) and CaSR (between 1.2 and 28.2 fold) gene expressions were observed in all COC groups. Successful differentiation of thyroid stem cells into Pt-like cells in coculture can be speculated to microenvironmental factors such as interaction of cells of the same embryological origin, exosomes, etc. Our results are promising in terms of solving the immune rejection problem together with the donor limitation in case of allogenous parathyroid transplantation.

ÖZET

KOKÜLTÜR ORTAMINDA TİROİD HÜCRELERİNİN PARATİROİD HÜCRELERİNE DÖNÜŞTÜRÜLMESİ

Paratiroid(Pt), kalsiyum ve fosfor homeostazını düzenleyen parathormonun (PTH) salgılanmasından sorumlu olan tek organdır. Vücuttaki birçok temel fizyolojik reaksiyon, bu homeostazın korunmasına bağlıdır. Serum kalsiyumundaki dengesizlik birçok metabolik soruna neden olur. Hipoparatiroidizm, serumda düşük PTH, düşük kalsiyum ve yüksek fosfat düzeyleri ile karakterize bir rahatsızlıktır. Hipoparatiroidizmde klasik tedavi kalsiyum ve D vitamini desteği ile sağlanır. Rekombinant insan PTH preparatları da kullanılabilir ancak maliyeti yüksek olduğu için çoğunlukla tercih edilmez. En etkili ve kalıcı tedavi seçeneği, paratiroid allo-transplantasyonudur (Pt allo-tx). Pt allo-tx'nda en büyük sorun uygun donör bulmak ve immun red cevabıdır. Bu sorunların aşılması için çeşitli doku mühendisliği çalışmaları yapılmaktadır ancak sorun halen tamamen çözülememiştir. Bu çalışmada embriyolojik kökeni paratiroidle aynı olan tiroid dokusunda yer alan kök hücrelerden kokültür ortamında paratiroid organoidi geliştirilmesi amaçlanmıştır. Dönüştürücü faktörler olarak Activin A ve sonic hedgehog (Shh) proteinleri kullanılmıştır. On dört günlük inkübasyondan sonra farklılaşma, qPCR kullanılarak gen ekspresyon profil analizi, biyokimyasal olarak PTH salgı ölçümü ve immunohistokimyasal analiz değerlendirmesi ile yapılmıştır. Oluşturulan kokültür organoidlerin gerçekte ölçülen PTH salım değerleri, beklenen PTH salım değerlerinden daha yüksek olarak ölçülmüş ve PTH salımında 2. gün ile 14. gün arasında istatistiksel olarak anlamlı artışlar gözlenmiştir. qPCR analiziyle, oluşturulan kokültür organoidlerin paratiroide özgü PTH ve CaSR gen ifadeleri incelenmiş ve tüm kokültür gruplarında PTH (4.0 ile 8.8 kat arasında) ve CaSR (1.2 ile 28.2 kat arasında) gen ifadelerinde artış gözlemlenmiştir. Tiroid dokusunda yer alan kök hücrelerin kokültür ortamında başarılı bir şekilde paratiroid benzeri hücrelere farklılaştırılması, aynı embriyolojik kökene sahip hücrelerin etkileşimi, eksosom gibi mikroçevresel faktörlere dayandırılabilir. Sonuçlarımız allojen Pt nakli yapılması halinde donör bulma sorunuyla birlikte immun red sorunun çözülebilmesi açısından ümit vericidir.

TABLE OF CONTENTS

LIST OF FIGURES

LIST OF TABLES

LIST OF SYMBOLS/ABBREVIATIONS

3D	Three dimensional
5-ALA	5-Aminolevulinic acid hydrochloride
CaSR	Calcium sensing receptor
COC	Coculture
DM	Differentiation medium
FBS	Fetal bovine serum
GCM2	Glial cell missing cells
H&E	Hematoxylin and eosin
HyperPTH	Hyperparathyroidism
HypoPTH	Hypoparathyroidism
PCR	Polymerase chain reaction
PGM	Parathyroid growth medium
Pt allo-tx	Parathyroid allo-transplantation
PTH	Parathyroid hormone
PTX	Parathyroidectomized
r-PTH	Recombinant human parathyroid hormone
RT	Room temperature
SGM	Standard growth medium
Shh	Sonic hedgehog
T	Thyroid
Pt	Parathyroid
TEC	Thymic epithelial cell
TGM	Thyroid growth medium
TMSC	Tonsil-derived mesenchymal stem cells
TTF1	Thyroid transcription factor 1

1. INTRODUCTION

1.1. PARATHYROID GLANDS

Parathyroid (Pt) is a pivotal organ of the endocrine system that regulates the calcium and phosphate metabolism by controlling the synthesis and secretion of parathyroid hormone (PTH). Parathyroid tissue was first described by an English anatomist Sir Richard Owen after performing necropsy on rhinoceros in 1852. In honor of his discovery it was named as "glands of Owen". He described that this newly discovered organ is yellow, compact glandular in structure and located adjacent to the thyroid (T) gland [1]. Later in 1880, a Swedish medical student Ivor Sandstrom discovered that Pt is present in various other animals including humans. After the anatomical and microscopic observations he thought that these structures would have been embryological remnants of thyroid so dubbed it as "glandulae parathyroidea''. He described the localization and the size of the organ as "found on both sides of the inferior border of the T and it is an organ with the size of a small pea". His examinations unfortunately were reported only on a local Swedish journal [2]. The significance of Pt remained uncertain until 1891. Then physiologist Eugéne Gley reported that total thyroidectomy performed on dogs resulted in tetany and death, on the other hand, animals could maintain their life in cases where Pts were not removed [3]. In 1909, two different research groups observed that the tetany and hypocalcemia due to thyroidectomy could be cured by either with calcium injection or Pt extracts [4,5]. These experiments, which can be regarded as the pioneer of Pt transplantation, were followed by the first autotransplantation of Pts performed by Anton von Eiselberg in 1982 [6]. Functionality and biochemical features became more clear with the discovery of the PTH by Collip in 1925 which further followed by the isolation and purification of PTH by Rasmussen and Craig in 1955 [7,8]. Studies demonstrating the vital function of this tiniest organ of human body have come a long way since 18th century through the present day. This study was carried out with the aim of contributing to the literature by creating therapeutic Pt-like structures that will secrete PTH.

1.1.1. Anatomy, Embryology, Histology

Pt glands, one of the most vital organs of endocrine system present in all vertebrates higher than fish. Anatomic localization of these glands is on anterior cervical region and attached to the posterior of T, another endocrine organ. A healthy human typically has two pairs of Pt glands as inferior and superior [9]. Each Pt gland is approximately 6 mm in length, 4 mm in width and 2 mm in thickness. All four Pt glands weigh around 120 mg in total [10]. Both anatomical localization and the number of glands may vary. Even though majority of the population have four glands, number of the glands can be ranged from 1 to 12. A study of 503 autopsies revealed that 17 percent of cases had more than four whereas 3 percent of the cases had less than four Pt glands [11]. Each bean-shaped Pt gland is separated from T by a thin fibrous capsule around it (Figure 1.1.). Translucent and grayish color of Pt glands of newborns turns into pale brown with age. There are many factors affecting the color of glands in the adulthood such as adipose volume, vascularization and cellular composition [12].

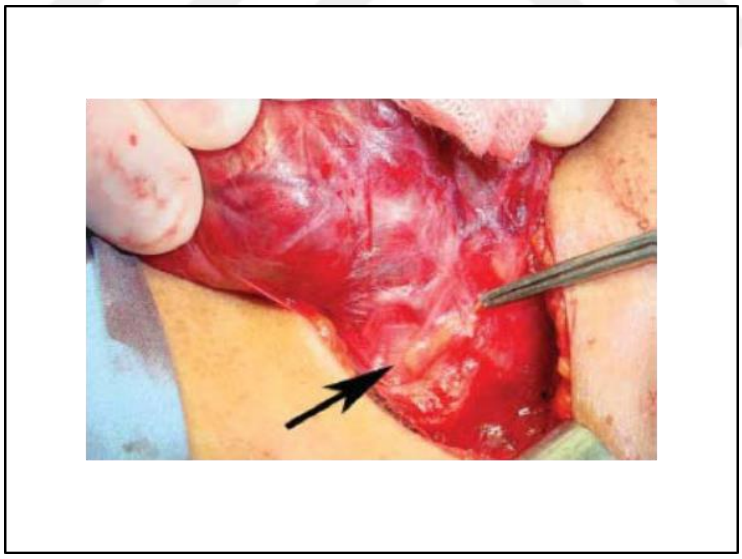

Figure1.1. Arrow showing the healthy Pt gland [13]

In embryonic development Pt glands, T and thymus are descended from paryngeal endoderm. Differentiation of these endocrine organs begins at the 5^{th} or 6^{th} weeks of gestation. While the superior Pt glands in pair originate from fourth pharyngeal pouches along with the T, the inferior Pt glands in pair originate from third pharyngeal pouches along with the thymus (Figure 1.2.). In general the Pt glands and their paryngeal pouch derivatives

of common embryological origin are anatomically close to each other [14,15]. On the contrary, ectopic Pt gland regions were reported in a variety of cases. The anatomical location of the inferior Pt glands has a higher incidence of ectopic occurrence when compared with superior Pt glands considering the longer migration route [16–18]. A significant meta-analysis on Pt surgery including 26 distinct studies with 7005 patients showed that the probability of having ectopic Pt gland is 15.9 percent. The highest proportion of those reported ectopic glands is located in neck followed by mediastinum [19].

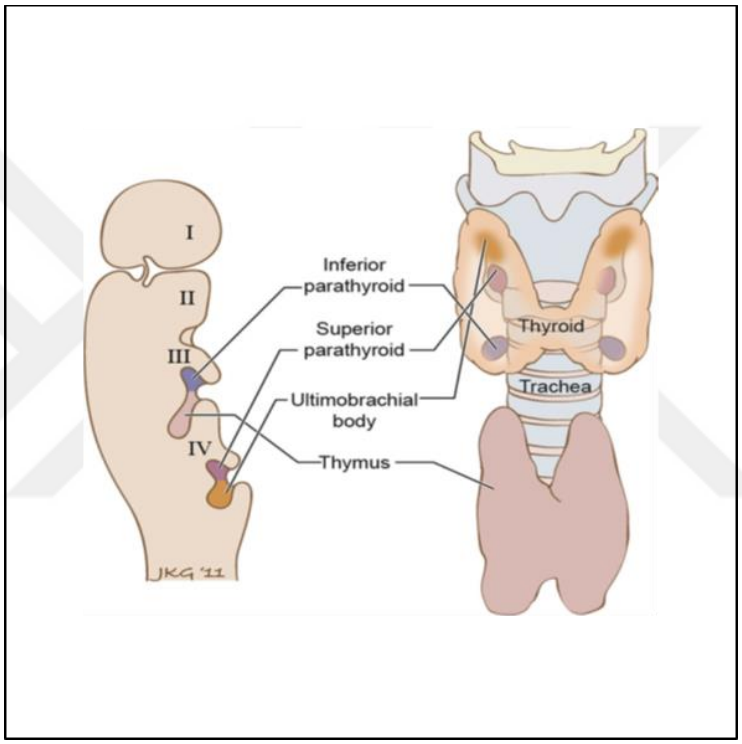

Figure 1.2. Anatomical illustration of Pt glands showing their embryological pharyngeal pouch origins [18]

Pt gland parenchyma is predominantly made up of two particular cell types as chief and oxyphil cells (Figure1.3.). In healthy human Pt glands the prevalence of chief cells with the function of PTH synthesis and secretion, are higher than oxyphil cells whose function have not been truly identified yet [20-22]. Only a few studies are present on the function of oxyphil cells as mentioned later in the text [23-25].

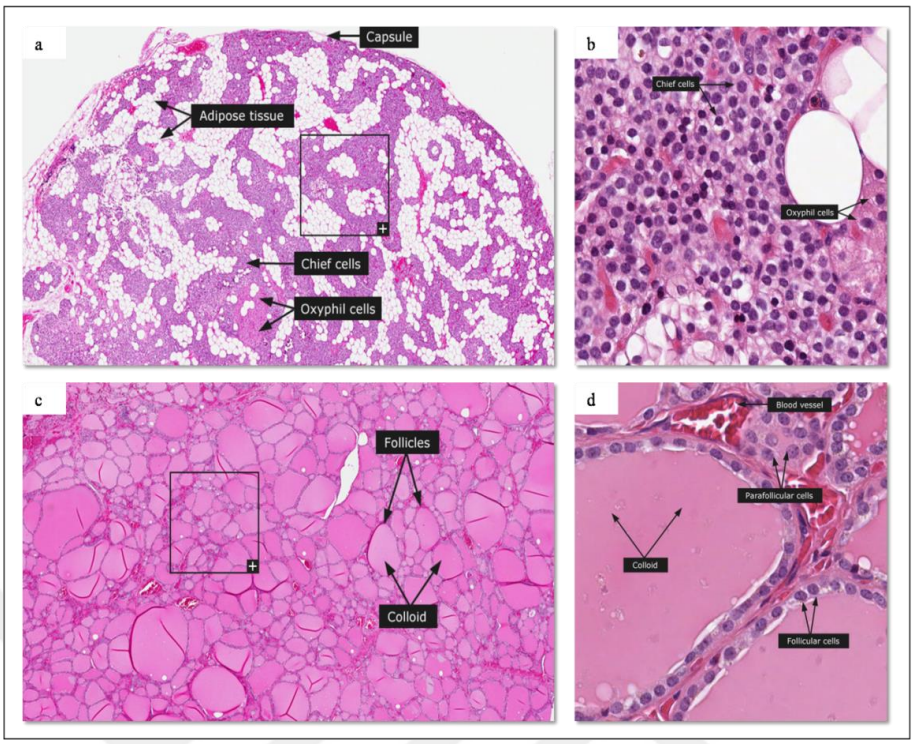

Figure 1.3. Histological representatives of Parathyroid(Pt) and Thyroid(T) (Haematoxylin and Eosin stained). (a) Pt capsule along with the two particular cell types as chief and oxyphil cells. (b) Differential staining of chief and oxyphil cells. (c) T comprised of follicles filled with colloid. (d) Specialized T cells as follicular and parafollicular cells [26]

Chief cells detect the serum calcium level with specific receptors called Calcium Sensing Receptor (CaSR) on its membrane to ensure the synthesis and secretion of PTH necessary for calcium homeostasis maintenance. These cells exhibit distinctive morphological characteristics during the secretory stages required for this homeostasis maintenance. The chief cells in the inactive stage contain scarce amounts of secretory granules with less developed organelles in their cytoplasm compared to the chief cells in the active stage. Furthermore, in contrast to the cuboidal morphological shape of the inactive cells, active cells demonstrates oval shape [27,28]. Oxyphil cells differ from chief cells in many aspects. While the size of oxyphil cells ranges from 12 to 20 μm, chief cells ranges from 6 to 8 μm. Histological studies revealed that greater amounts of mitochondria present in cytoplasm of oxyphil cells when compared to chief cells and thus their cytoplasm is more eosinophlic [29]. Considering higher abundance of mitochondria, oxyphil cells demonstrate greater oxidative and hydrolytic enzyme activity. For instance, Vitamin D 1 hydroxylase expression

is high in these cells as vitamin D metabolism takes place in the mitochondria of oxyphil cells [24]. Early studies suggested that oxyphil cells were metabolically inactive degenerated chief cells. However, investigation of cells with average characteristics among cytoplasmic features of chief and oxyphil cells reveals that they are chief cells' derrivatives. This derivation occur naturally due to aging or might be as a result of metabolic instabilities [22]. Also PTH and Glial Cell Missing 2 (GCM2) expressions are both present on oxyphil and chief cells. Despite all these findings, the function and origin of the oxyphill cells is rather controversial [24,30].

1.1.2. Physiology

Pt glands are responsible for the regulation of serum ionized calcium (Ca^{2+}) and phosphorus levels through PTH synthesis and secretion. Initially alterations in serum Ca^{2+} concentrations are sensed by CaSR on chief cells of Pt. In hypocalcemic situations, meaning low level of the serum Ca^{2+}, secretion of PTH is stimulated as the binding of Ca^{2+} to CaSR in the Pt decreases. Circulating PTH acts to restore homeostasis by increasing Ca^{2+} via various mechanisms work collaboratively in the bone, kidney and small intestine. The release of calcium from bone to bloodstream is provided by the PTH stimulated osteoclasts. As a catabolic effect, osteoclast activity increases bone resorption which in turn increase the serum Ca^{2+} levels. In kidneys PTH directly augments Ca^{2+} re-absorption. Moreover, inactive vitamin D (25-hydroxyvitamin D_3) in the kidneys is converted into active vitamin D (1,25-dihydroxyvitamin D_3 ($1,25(OH)_2D_3$)) by PTH catalysis. Active vitamin D, which acts as a co-factor in the small intestine, provides the intestinal absorption of dietary calcium. Additionally, Ca^{2+} resorption from bones is also promoted by active vitamin D when it is in cooperation with PTH. When serum Ca^{2+} reaches its normal range (1.1–1.4 mmol/L) in the circulation, further PTH secretion is inhibited due to activation of CaSR [13,31].

1.1.3. Diseases of the Parathyroid Gland

Many physiological events in the body depend on the maintenance of the calcium and phosphorus homeostasis regulated by secretion and release of PTH from Pt glands. While bone mineralization, blood coagulation, muscle fiber contraction, neurotransmitter release, enzymatic activity regulation and cell signaling needs calcium; preservation of membrane integrity, intracellular signaling through phosphorylation of various enzymes, formation of the backbone of nucleic acids, and cellular metabolism (ATP production) need phosphorus [32]. The homeostatic imbalance in these minerals leads to Pt disorders such as Pt cancer, hyperparathyroidism (HyperPTH) and hypoparathyroidism (HypoPTH). For diagnostic investigations of these diseases, serum based methods such as serum PTH, serum phosphorus, serum calcium level measurements are predominantly used.

While Pt cancer is extremely rare, HyperPTH is the main disease of the Pt glands. HyperPTH is characterized by an excess PTH secretion. High level of PTH secretion causes impairments in calcium metabolism leading to reduction in bone density and improper signal transmission within nerve cells. It's prevalence seems to be age-related with the highest occurrence rates by age 55 [33]. Additionally 3-4 fold greater incidence is observed among women than men [34]. The incidence also varies among populations. In some studies, this frequency has been reported as 2-4 in 10,000 people whereas 80-90 in others [34,35]. HyperPTH can be categorized under three main types as primary, secondary and tertiary. In primary HyperPTH, excess PTH secretion arises due to the intrinsic abnormal pathology. Almost 85 percent of the cases with primary HyperPTH have adenoma induced overproduction of PTH. This is followed by cases with hyperplasia of the Pt gland (13 percent) or carcinoma (1 percent) [36]. Although cases are generally asymptomatic, most prevalent clinical manifestations are nephrolithiasis, join/bone pain, muscle weakness, fatigue and depression [37]. Secondary HyperPTH is characterized by high serum PTH levels associated with chronic kidney diseases, vitamin D deficiency, calcium deficiency or malabsorption. When prolonged secondary HyperPTH causes permanent secretion of PTH and hypercalcemia, it was termed as tertiary HyperPTH [38]. The most common and accurate treatment for HyperPTH is subtotal parathyroidectomy which is surgical removal of Pt gland. Although in most cases parathyroidectomy is curative, calcimimetrics are used for the management of patient groups who are not suitable for surgery [39].

Permanent HypoPTH with prevelance of 1–3 in 10,000 people, is a relatively rare condition when compared to HyperPTH. It includes congenital, autoimmune and acquired (most often as a result of post-operative complication related to surgical malpractice of thyroidectomy) types [40]. Most often cause of permanent HypoPTH is complication of thyroidectomy. As opposed to HyperPTH, clinical symptoms are related to low serum level of PTH. Inadequate amount of PTH secretion in turn leads to hypocalcemia and hyperphosphatemia. Typical clinical manifestations are neuromuscular hyper excitability including tetany, muscle cramps, tingling, Trousseau and Chvostek' signs [41]. Patients might also present premature cataracts, cardiac arrhythmias, basal ganglia calcifications and cognitive dysfunctions [42]. Oral or intravenous calcium and vitamin D supplements are given to the patients to reduce HypoPTH symptoms. However, medication approaches are not therapeutic but only used for symptomatic relief. Moreover medical administrations acquire many side effects in consequense of consistent daily intake and high dose requirements [43]. Depending on these limitations, studies have been carried out on synthetic drug designs that can functionally replace PTH produced by Pt glands. Studies revealed that recombinant human PTH (r-PTH) preparations which are alternative to conventional medication, present fewer side effects. For example teriparatide (Forteo®), FDA approved synthetic PTH drug, presents less side effects with improved quality of life, however, it still has its own drawbacks [42,44]. Toxicologic studies revealed that teriparatide causes increased risk of osteosarcoma in rats due to long-term usage. Hence the recommended duration of synthetic PTH analogs, medication is restricted to 24 months [45]. In addition, patients have limited access to r-PTH preparations as they are more expensive than drugs used in conventional therapy [46]. The most effective, physiologic and life long maintenance treatment option of permanent HypoPTH is Pt allo-transplantation (Pt allo-tx). In this treatment surgically removed hyperplastic Pt tissues are used as an allograft to the patient who has a permanent HypoPTH. Unfortunately, there are two major problems in Pt allo-tx: finding a proper donor and immune rejection of transplanted allograft cells [47].

1.2. TISSUE ENGINEERING

Tissue engineering is an emerging interdisciplinary field in which integration of engineering and life science approaches used for the development of functional biological substitutes. The main purpose is to obtain biological substitutes that have the ability to repair, replace or improve the function of damaged tissue or entire organ [48]. Although the first successful human organ transplantation occurred in 1954 by Thomas Murray, the replacement of damaged or dysfunctional organs idea dates back to the ancient times. The first known written sources about organ transplantation is the instructions of Samhita, an Indian physician believed to be lived in about 6th B.C. In these instructions, reconstruction of the facial injuries by transplanting an autogenous skin flap was described. Then a famous Italian surgeon named Gasparo Tagliacozzi, renovated Samhita's skin autograft technique and the technique consecutively was referred as the ''Italian method'' by the 16th century [49,50]. Later, vascular reconstruction strategies devised by Alexis Carrel with the aim of restoring normal blood circulation gave rise to a scientific breakthrough in transplantation studies [51].

Modern medical developments since the beginning of 20th century have transformed organ transplantation into a routine treatment for patients with organ failure. Transplantation can be subclassified depending on the organ replacement strategies, as autografts, allografts, and xenografts. These three strategies have their own drawbacks associated with the risks involved. Autograft technique, which is the transplantation of one's own tissue/organ without the demand for an HLA-matched donor, is considered advantageous because it provides rapid graft incorporation without immune rejection. On the other hand, additional surgical operations, higher risk of post operative infections, insufficient tissue quantity and donor site morbidity can be listed as it's drawbacks. Allograft, describing tissue transplantation within the same species from a genetically distinct donor has other usage restictions due to the histocompatibility of graft with immune rejection risk and viral or bacterial disease transmission between individuals. Besides xenografts which is transplantation in between species with the distinct genetic makeup exhibit limited usage regarding ethical issues [52-54]. The need for implementing novel techniques has been observed by scientific communities due to the growing number of patients registered on transplant waiting lists and the shortage of available organs for transplantation. The emergence of new research areas and related discoveries in the field of tissue engineering, which brings life and engineering

sciences together, has also dramatically transformed and improved the technologies produced to overcome the obstacles in organ transplantation. In the light of scientific developments in tissue engineering techniques, which are mostly based on scaffolds, stem cells and growth factors, a wide variety of methods have been invented that allow the reconstitution of functional biological substitutes *in vitro*. The transfer of these biological substitutions from the experimental stage to therapeutic applications over time will create an alternative to traditional organ transplantation and contribute to the solution of transplantation-related problems [55].

1.2.1. Parathyroid Related Tissue Engineering Studies

To date, numerous studies have attempted to establish Pt-like cells by applying different tissue engineering approaches. Bingham *et al.* differentiated human embryonic stem cells (hESC) into Pt-like cells by the utilization of a conditioned medium containing specific growth factors. Bingham protocol was a renovated version of D'Amour protocol which enabled hESCs to differentiate into endodermal cells. In this renovated protocol, undifferentiated hESCs were seeded on a feeder layer and grown in a modified medium that comprised low dose of Activin A with Fetal Bovine Serum (FBS) in increasing proportions for the first five days. When transformation of regular hESC morphology to cuboidal cells growing in monolayer was observed, cells were dispersed and replated. For further differentiation, conditioned medium application was carried out for an additional 7 days with 5 percent FBS and Activin A. Although Pt tissue specific gene expressions (CXCR4, GCM2, CaSR, PTH and Sox17) revealed that the human embryonic stem cells were differentiated into Pt-like cells, PTH release was not measured in this study. PTH release was only achieved by keeping Pt specific gene-expressing cells in an Activin A-free culture for an additional two weeks [56]. In repeated experiments of the same group with a different hESC line, it was observed that the usage of Shh also promoted Pt-like cell differentiation [57]. A broader perspective was adopted after these two significant studies in which hESC lines were used as a culture model in the differentiation protocol optimization. Based on these studies, differentiation protocol was optimized and Sonic Hedgehog (Shh) was included in addition to Activin A [56,57]. In a later study, optimized Pt differentiation protocol was carried out with thymic epithelial cell (TEC) isolated from thymus in order to avoid hESC related alloimmunologic hurdles and the potential teratoma formation risk. Initial target of this study

was to identify the differentiation capacity of thymus which has embryogenically same origin with Pt. Observation of PTH, CaSR, CXCR4 and GCM2 marker expressions and PTH secretion in differentiated cells demonstrated that Pt differentiation from autologous precursor cells could be achieved [58].

Also several studies have used mesenchymal stem cells to create Pt-like cells. Firstly, promising results were obtained using tonsil-derived mesenchymal stem cells (TMSC). Isolation of the TMSC from the excised tonsil tissues of multiple donors achieved with collagenase type I and DNase. Pt specific gene expressions (CaSR, GCM2 and PTH) were observed after differentiation of cells for 7 days with the Bingham protocol including Shh and Activin A [59]. Park *et al.* took their work to the next level by creating 3D cultures using TMSC derived Pt-like cells embedded in matrigel. It was also the first study to test *in vivo* restoration capacity of the differentiated TMSCs. They generated a parathyroidectomized (PTX) rat model. Prior to surgery, injection of 5-aminolevulinic acid hydrochloride (5-ALA) into peritoneum performed for photodynamic Pt detection. Evaluation of 3D structures of TMSC derived Pt-like cells was assessed by the injection of the differentiated cells alone or implantitaion of the cells after embedded in matrigel to the PTX rats. It was demonstrated that matrigel embedded TMSC have improved survival rates with higher PTH release [60]. However, as matrigel is not clinically feasible in human due to its tumor cell origins, researchers attempted to create scaffold free 3D cultures or biocompatible scaffolds [61]. Scaffold-free TMSC spheroids were generated in a concave polydimethylsiloxane microwell plate and *in vivo* Pt functions were evaluated by the subcutaneous injection to PTX rats. Compared with the previous study of the same group, it was observed that Pt functionality was preserved over a longer period of time as 3 months when scaffold-free TMSC spheroids were injected [62].

Jung *et al*. used plasma gel as an autologous 3D scaffolding material instead of matrigel. TMSC derived Pt-like cells were fabricated with the plasma gel and afterwards injected intramuscularly to dorsum of PTX rats. Immunohistochemical and immunofluorescent staining results confirmed Pt-like cell features in the TMSC plasma gel implantation sections [63]. To prevent foreign body rejection after transplantation, the researchers also tried to encapsulate the Pt tissue with various biocompatible materials. Lee *et al*. examined *in vitro* and *in vivo* functionality of the microensapsulated hyperplastic Pt tissues. In this study three-layer structure that composed of alginate, photosensitive poly (L-lysine) and short chain

alginate-co-MPEG was used in microcapsule preparation. They have reported that microencapsule transplanted PTX rats were normocalcemic despite the absence of immunosuppressive drug administration [64]. Other researchers have used Pt adenoma or hyperplasia tissue from 46 patients to construct a microphysiological system with anintegrable pseudogland model that would recapitulate the physiological characteristics of the Pts. Free-floating pseudoglands were generated after culturing patient derived Pt cells into non-adherent plates. CaSR expression, PTH secretion along with the histological Hematoxylin and Eosin (H&E) staining results revealed that constructed pseudoglands show Pt-like cell characteristics, thus can be used in development of potential treatment in HypoPTH [65]. In more recent studies, adipose-derived stem cells (ADSCs) isolated from rats and humans were used as a source for Pt-like cell differentiation [66,67]. Differentiation of isolated rat ADSCs into Pt-like cells were induced by Shh and Activin A. The effect of distinct Activin A concentrations on differentiation was examined by keeping the amount of Shh constant at 100 ng/mL. As a result, optimized concentration of Activin A was determined as 75 ng/mL. Significant increases in the mRNA and protein levels of Pt markers of CaSR, PTH, and GCM2 were recorded after performing the differentiation induction procedure for 21 days. Another study with a similar methodology was successfully conducted with the human ADSCs isolated from subcutaneous abdominal adipose tissue [67]. Other tissue engineering approach based on the differentiation of induced pluripotent stem cells into Pt-like cells was first demonstrated experimentally by Lawton *et al.* in 2020 [68]. When treatment with certain basal media (RPMI, High Glucose DMEM, DMEM-F12) were tested, it was concluded that the optimized media depended on the differentiation phase of the cells.

1.3. AIM OF STUDY

The aim of this study is to differentiate Pt-like cells from T stem cells in a coculture environment. Due to common embryonic origin and close anatomical relationships, varying concentrations of hyperlastic Pt and healthy T cells were cocultured to observe the effect of microenvironment on Pt differentiation and Pt-like organoid functionality. Differentiation was induced by the utilization of a conditioned medium containing specific growth and differentiation factors, such as Shh and Activin A. Pt transplantation should be performed in the allotype. However, post-transplant immune rejection reaction is commonly observed despite weak HLA expression of Pt cells. In addition, the conceptual absence of immunosuppressive drug use in Pt allotransplantation (Pt allo-tx) poses a risk of immune rejection reactions. Moreover, since the cells used in Pt allo-tx are hyperplastic cells, it is difficult to find donors with HyperPTH. Besides, preparing cells for transplantation is a difficult task and requires special laboratory conditions and experienced staff. If we succeed in differentiating the T cells into Pt cells, immune rejection reaction and finding a suitable donor problems will be solved by using autogenous T cells of the patient.

2. MATERIALS AND METHODS

2.1. MATERIALS

2.1.1. Consumables

Table 2.1. Consumables used in experiments

Item	Brand	Catalog No
1.5 mL Eppendorf Tubes	Axygen	MCT-150-A
Stripette™ 5 mL Serological Pipets, Polystyrene	Corning	356543
Falcon® 10 mL Serological Pipet, Polystyrene	Corning	356551
Falcon® 25 mL Serological Pipet, Polystyrene	Corning	356525
Ultra-low Attachment Multiwell Plates (96-well format, U shape)	Corning	#4520
Capp Sharp Reagent Rreservoir 10 mL	Capp	CA40515
Cell strainer (40 μm)	Falcon®	352340
3 Well Chamber, removable	Ibidi	80381

2.1.2. Chemicals

Table 2.2. Chemicals used in experiments

Item	Brand	Catalog No
DMEM/F12 Medium	Gibco	10565-018
RPMI 1640 Medium, GlutaMAX™ Supplement	Gibco	61870036
Nutrient Mixture F-12 Ham (Coon's modification)	Sigma	F6636
FBS, Qualified HI	Gibco	10500-064
DPBS 1X	Gibco	14190-169
Trypsin-EDTA (0.25 percent), phenol red	Gibco	25200056
Anti-Parathyroid Hormone Receptor 1/PTH1R antibody	Abcam	ab75150
Anti-CaSR antibody	Abcam	ab137408
Anti-Chromogranin A antibody	Abcam	ab45179
Anti-TTF1 antibody [8G7G3/1] (ab72876)	Abcam	ab72876
Anti-TSH Receptor/TSH-R antibody (ab202960)	Abcam	ab202960
Goat Anti-Rabbit IgG H&L (Alexa Fluor® 488)	Abcam	ab150077
Goat anti-Mouse IgM Cross-Adsorbed Secondary Antibody, DyLight 594	Invitrogen	SA5-10152
Recombinant Human/Mouse/Rat Activin A Protein R&D	R&D Systems	338-AC-050
Recombinant Human Sonic Hedgehog/Shh (C24II) N-Terminus	R&D Systems	1845-SH-100
DNase I, grade II, from bovine pancreas	Roche – Merck	10104159001
Collagenase Type II	Gibco	17101015
Collagenase Type IV	Gibco	17104-019
Transferrin	Sigma	T8158-100MG

Somatostatin	Sigma	S1763-1MG
Hydrocortisone	Sigma	H0888-1G
Gly-His-Lys acetate salt	Sigma	G7387-.5MG
Thyrotropic hormone from bovine pituitary	Sigma	T8931-1VL
ITS + Premix	Corning	354352
Alexa Fluor™ 647 Phalloidin	Invitrogen	A22287
DAPI	Sigma-Aldrich	28718-90-3
10X TBE Electrophoresis Buffer	Thermo Fisher, USA	00776829

2.1.3. Kits

Table 2.3. Kits used in experiments

Item	**Brand**	**Catalog No**
LIVE/DEAD™ Viability/Cytotoxicity Kit, for mammalian cells	Invitrogen	L3224
Human PTH ELISA Kit	Abcam	ab230931
Nucleospin RNA XS Isolation Kit	Macharey-Nagel(M-N)	740902,5
iScript™ cDNASynthesis Kit	Bio-Rad	1708891
iTaq Universal SYBR Green Supermix (2X)	Bio-Rad	1725120
PKH26 Red Fluorescent Cell Linker Kit for General Cell Membrane Labeling	Merck	PKH26GL
Vybrant™ DiO Cell Labeling	Invitrogen	V22886

2.1.4. Instruments

Table 2.4. Instruments used in experiments

Item	Brand
Biological Safety Cabinet	Biobase
Cell Culture Incubator	Esco
Centrifuge	Gyrozen
Water bath	N-Biotek
Light Microscope	Carl Zeiss, Germany
Confocal Microscope(LSM 700)	Carl Zeiss, Germany
Fluorescent Microscope (Axio Vert.A1)	Carl Zeiss, Germany
ChemiDOC XRS+Gel Imaging System	Bio-Rad
NanoDrop Spectrophotometer (Nanodrop 2000)	ThermoFisher, USA
Elisa Plate Reader (Elx800)	Bio-Tek, USA

2.2. CELL ISOLATIONS

In this study human parathyroid and human thyroid tissues were provided by Yeditepe University Hospital, Department of Endocrine Surgery unit. Local human ethics committee approved the methodology of this research and informed consent from the patients were obtained before starting to the study. (Local ethics committee (Turkish Ministry of Health, General Directorate of Health Services, no:56733164/203))

Patient with HyperPTH due to chronic renal failure was operated for subtotal parathyroidectomy. During operation nearly 6 cm^3 of Pt tissue was excised from the patient with secondary HyperPTH and 2 cm^3 of the excised tissue was separated and transferred into a sterile falcone tube including harvest medium (Dulbecco's Modified Eagle Medium with 1,000 unit/mL Penicillin-Streptomycin). Then, it was transported on ice to the University Thyroid, Parathyroid and Organoid Laboratory. T tissue was excised from a patient who underwent total thyroidectomy due to the diagnosis of nodular goiter. A tissue piece with a volume of 2 cm^3 taken from the healthy parenchyma of T that does not contain nodules was transferred to the laboratory with the same protocol. Cell isolations from Pt and T were applied with the protocols described in following cell isolation from human parathyroid tissue and cell isolation from human thyroid tissue subtitles.

2.2.1. Cell Isolation From Human Parathyroid Tissue

Pt tissues were first mechanically disrupted in a petri dish containing sterile 1X Phosphate buffer saline (PBS). Firstly, tissue was minced into smaller pieces via scissors. Then gland capsule, fat and connective tissues were trimmed and removed from the tissue with the help of scalpels. After achieving mechanical disintegration, PBS was removed from the petri dish and then washed with 1X PBS again before enzymatic digestion. Minced tissue pieces were taken into the fresh enzyme solution containing Collagenase Type II, DNase I and BSA at a concentration of 1 mg/mL, 0.05 mg/mL and 5 mg/mL, respectively. Afterwards it was shaken at a constant speed of 80 rpm in a water bath at 37ºC for 40 min. Mechanic fragmentation was performed via serologic pipettes in every 10 min. At the end of 40 min of shaking, tissue pieces were settled down with centrifugation at 500 rpm for 5 min. Then the supernatant was filtered through a 40 μm cell strainer and 40 ml of fresh medium was

added onto it. Afterwards it was centrifuged at 2300 rpm for 5 min. The pellet was resuspended in fresh standard growth medium (RPMI 1640 medium containing 10 percent FBS and 1 percent P/S). The same process was repeated until all the remaining tissue pieces were treated with fresh enzyme solution and centrifuged at 2300 rpm for 5 min. Afterwards isolated Pt cells were seeded in an appropriate culture flask after counting with hemocytometer.

2.2.2. Cell Isolation From Human Thyroid Tissue

T tissues were first mechanically disrupted in a petri dish containing fresh and sterile 1X PBS. First tissue was minced into smaller pieces via scissors. Then fat and connective tissues were removed from T tissue with the help of scalpels. After achieving mechanical disintegration, PBS was removed from the petri dish and then washed with 1X PBS again before enzymatic digestion. Minced tissue pieces were taken into fresh enzyme solution containing Collagenase Type IV and DNase I at a concentration of 1 mg/mL and 0.1 mg/mL, respectively. Afterwards it was shaken at a constant speed of 80 rpm in a water bath at 37ºC for 40 min. Mechanic fragmentation was performed via serologic pipettes in every 10 min. At the end of 40 min of shaking, tissue pieces were settled down with centrifugation at 500 rpm for 5 min. Then the supernatant was filtered through a 40 μm cell strainer and 40 ml of fresh medium was added onto it. Afterwards it was centrifuged at 2300 rpm for 5 min. The pellet was resuspended in fresh standard growth medium (RPMI 1640 medium containing 10 percent FBS and 1 percent P/S). The same process was repeated until no tissue remained and cells were centrifuged at 2,300 rpm for 5 min. The supernatant was removed and pellet was incubated in erythrocyte lysis buffer for 10 min at 37°C in 80 rpm shaking water bath. After centrifugation, supernatant was removed. Then the pellet was resuspended in fresh standard growth medium. Isolated T cells were seeded in an appropriate culture flask after counting with hemocytometer.

2.3. GENERATION OF 3D ORGANOIDS

To establish three dimensional organoids, enzymatically isolated T and Pt cells were seeded in an ultra-low attachment multiwell plates at a constant density of total 20,000 cells per well. The COC organoid groups were established with different proportions of Pt and T cells so as to determine the optimal ratio required for Pt-like differentiation. Performed Pt and T cell ratios were 1:1, 1:2, 1:4, 1:8 and 1:16 (Pt:T) for the COC organoid generation. Initially all organoids were seeded in a standard growth medium (SGM). The generated organoid groups and their specified growth mediums were indicated in Table 2.5.

Table 2.5. Overview of established organoid groups with different growth media

Generated Organoid Groups	**Growth Medium**
Only Thyroid	Thyroid Growth Medium (TGM)
Only Parathyroid	Parathyroid Growth Medium (PGM)
COC 1:1 (Pt:T)	Differentiation Medium (DM)
COC 1:2 (Pt:T)	Differentiation Medium (DM)
COC 1:4 (Pt:T)	Differentiation Medium (DM)
COC 1:8 (Pt:T)	Differentiation Medium (DM)
COC 1:16 (Pt:T)	Differentiation Medium (DM)

2.4. ORGANOID MAINTENANCE

On the second day, SGM was replaced with specific culture medium containing the required supplements as seen in Table 2.6. All plates were placed in a humidified incubator set to 37°C and 5 percent CO_2. For the maintenance of organoids, fresh medium was added at least every third day. All generated organoid cultures were maintained up to 14 days.

Table 2.6. The overview of the applied growth medium compositions

Growth medium	Component	Concentration	Company
SGM	RPMI 1640	1 X	Gibco, Invitrogen, USA
	Fetal Bovine Serum (FBS)	10 percent (v/v)	Gibco, Invitrogen, USA
	Penicillin/Streptomycin	100 U/mL	Pan Biotech, Germany
TGM	Coon's Modification Of Ham's F-12 Medium	1 L	Sigma-Aldrich, USA
	Fetal Bovine Serum (FBS)	5 percent (v/v)	Gibco, Invitrogen, USA
	Human Recombinant Insulin	10 μg/mL	Sigma-Aldrich
	Hydrocortisone	10 nmol/L	Sigma-Aldrich
	Human Transferrin	5 μg/mL	Sigma-Aldrich
	Gly-His-Lys Acetate Salt	10 ng/mL	Sigma-Aldrich
	Somatostatin	10 ng/mL	Sigma-Aldrich
	Penicillin/Streptomycin	100 U/mL	Pan Biotech, Germany
PGM	DMEM/Ham's F-12	500 mL	Gibco, USA
	ITS Premix	1 percent	Corning, USA
	Penicillin/Streptomycin	100 U/mL	Pan Biotech, Germany
DM	RPMI 1640	500 mL	Gibco, Invitrogen, USA
	Fetal Bovine Serum (FBS)	5 percent (v/v)	Gibco, Invitrogen, USA
	Activin A	100 ng/mL	R&D Systems, USA
	Sonic Hedgehog	100 ng/mL	R&D Systems, USA
	Penicillin/Streptomycin	100 U/mL	Pan Biotech, Germany

2.5. LIVE/DEAD VIABILITY ASSAY

Cell viability of organoids was assessed by using Live/Dead® Viability/Cytotoxicity Kit (Invitrogen, USA) on days 7 and 14. According to the manufacturers' instructions, assay solution was prepared by combining 2 μM Calcein-AM and 4 μM ethidium homodimer-1 in 1X PBS. Organoid cultures were rinsed with 1X PBS after the removal of medium in each well. Then organoid cultures were incubated with the prepared assay solution for 35 min in the dark. Upon incubation, assay solution was discarded gently without damaging the samples and washed with 1X PBS. Afterwards visualization of live and dead cells of the organoids was performed under florescence microscope and images were recorded in TIFF format.

2.6. CELL CHARACTERIZATION

Isolated Pt and T cells' morphology were investigated for their characterization. Adequate amounts of cells were taken from the isolated cells prior to organoid formation and seeded separately into flasks as monolayer culture for morphologic characterization. Isolated cells were grown in their basal mediums as PGM for Pt cells and TGM for T cells (Table 2.6.). They were maintained viable under standard cell culture conditions at 37°C and 5 percent CO_2 for 96h. Cellular morphology was imaged under bright-field (BF) microscopy and recorded in TIFF format. For further characterization of the isolated cells, specific protein markers were detected by immunofluorescence staining.

2.6.1. Cellular Morphology Assessment of Isolated Cells

Isolated T and Pt cells (1×10^3 cells/well) were separately seeded onto a 3-well chamber slide (Ibidi) with 2 ml of appropriate medium as TGM or PGM. Seeded cells were incubated for 96 h for the attachment and proliferation. Cellular morphology of the isolated cells were observed under BF microscopy without fixation.

Immunofluorescence staining of the isolated cells was carried out to examine cell specific marker proteins. The primary and secondary antibodies used for immunofluorescence were rabbit polyclonal anti-CaSR antibody (Abcam, ab137408; 1:500), rabbit polyclonal anti-

Parathyroid Hormone Receptor 1/PTH1R antibody (Abcam, ab75150; 1:500), rabbit polyclonal anti-Chromogranin A antibody (Abcam, ab45179; 1:50), rabbit polyclonal anti-Thyroid Stimulating Hormone Receptor/TSH-R antibody (Abcam, ab202960; 1:500), rabbit monoclonal anti-PAX8 antibody [EPR18715] (Abcam, ab191870; 1:1,000), rabbit monoclonal Anti-TTF1 antibody [SP141] (Abcam, ab227652; 1:25), rabbit polyclonal Anti-FOXE1 antibody (Abcam, ab236661; 1:200), mouse monoclonal anti-Parathyroid Hormone antibody [rPTH/911] (Abcam, ab234415; 1 µg/mL), goat anti-Mouse IgM Cross-Adsorbed Secondary Antibody (DyLight 594) (Invitrogen, SA5-10152; 1:200) and goat anti-Rabbit IgG H&L (Alexa Fluor® 488) (Abcam, ab150077; 1:1,000). Also, Alexa Fluor™ 647 Phalloidin (Invitrogen; 1:1,000) was used for the cytoskeleton staining whereas DAPI (Sigma-Aldrich; 1 µg/mL) was used for the nuclei staining.

Isolated cells were fixed in 3.7 percent formaldehyde at room temperature (RT) for 30 min. Permeabilization with 0.1 percent Triton X-100 in 1X PBS for 5 min at RT was applied only for the internal protein detection. Following fixation and/or permeabilization, cells were rinsed with PBS and blocking was performed with 3 percent FBS in PBS for 10 min in order to reduce the non-specific staining. Afterwards cells were again rinsed with 1X PBS a few times. Incubation of the isolated cells with the primary antibodies for 1 h at RT was then followed by the addition of appropriate secondary antibodies for 1 h at RT. During incubation with antibodies, samples were protected from light exposure. Cells were again washed using 1X PBS after incubation to remove unbound conjugates. Also, for nuclei detection, DAPI was incubated for 15 min at RT. Minimizing the photobleach after staining was achieved by the addition of antifade mountant (Invitrogen, Thermo Scientific, USA). Visualization was performed by confocal microscopy with the fitting filters.

2.7. CELL LABELING

Prior to COC organoid generation, isolated T and Pt cells were individually labeled with fluorescent dyes for the estimation of organizational assembly. To track thyroid in COC organoids, T cells were labeled with VybrantDiO, a cell surface-labeling green fluorescent dye having excitation/emission values of 484/501 nm. To track parathyroid cells in COC organoids, Pt cells were labeled with PKH26, a cell surface-labeling red fluorescent dye having excitation/emission values of 551/567 nm. Labeling was performed according to the

manufacturer's instructions. Initially T cells were washed with serum-free medium. VybrantDiO cell labeling solution was diluted 1:200 with 1X PBS and added on the suspended T cells. Incubation lasted for 20 min at 37°C and then cells were washed a few times using complete medium. For Pt labeling, PKH26 cell labeling solution was diluted with buffer C. Cells were then incubated with diluted dye solution for 3 min at RT. Then 2 mL of FBS was added on the suspended Pt cells in order to terminate the labeling reaction. Following 1 min of incubation with FBS, cells were washed a few times using complete medium. Visualization was performed by confocal microscopy with the fitting filters.

2.8. IMMUNOHISTOCHEMICAL ANALYSIS

Generated organoids were previously fixed in 10 percent formalin for at least 24 h. Low melting agarose solution (4 percent) was prepared gently by adding agarose powder in 1X PBS without forming any clumps. The solution was prepared on a magnetic stirrer at 50ºC for 30 min and then microwaved for complete homogenization. Afterwards, 10 percent formalin fixed organoid samples were embedded in agarose. Polymerization of agarose solution was achieved after 15 min of incubation. Agarose-embedded specimens were then transferred to a tissue culture plate and transported on ice to pathology laboratory of Yeditepe University Hospital. Specimens were then embedded in parafin and sectioning was done by using microtome. Primary antibodies against calcium sensing receptor (CaSR), parathyroid hormone (PTH) and thyroid transcription factor 1 (TTF1) were used for immunohistochemical characterization. Sectioned tissues (4 mm) were stained with an automated immunohistochemical stainer (Leica® BOND-MAX) and manufacturer’s instructions were followed in this procedure. Detection was performed with the BOND Polymer Refine Detection Kit (Leica® DS9800). In addition hematoxylin and eosin (HE) stainings were applied to organoid sections.

2.9. BIOCHEMICAL ANALYSIS

To determine whether the generated organoids were functional, biochemical analysis was carried out by PTH measurement. Culture media of each organoid groups (total amount of collected media from 10 wells for each group was ≈1ml) were transferred to eppendorf tubes

at determined time intervals as day 2, day 7 and day 14 and stored at -80 ℃ until further use. Also, specific media used in culturing (TGM, PGM, DM) were transferred to eppendorf tubes for blank subtraction. Prior to PTH measurement, mediums were thawed and centrifuged at 10,000 rpm for 5 min. Then supernatants were taken to the new eppendorf tubes. PTH secretion was measured with PTH ELISA kit after the transfer of the collected media to Biochemistry Department of Yeditepe University Hospital.

2.10. TOTAL RNA ISOLATION

Differentiation capacity of the COC organoids were evaluated by quantitative polymerase chain reaction (qPCR). For this purpose firstly, total RNA was isolated from organoid cultures subsequent to 14 days of incubation. NucleoSpin® RNA XS isolation kit (MN, Germany) was used and manufacturer's instructions were followed in this procedure. Organoid samples were lysed and homogenized with 100 µL Buffer RA1 and 2 µL TCEP and mixed vigorously by vortex. Then 5 µL carrier RNA working solution (20 ng) was added and again mixed. Addition of 100 µL ethanol (70 percent) to the homogenized lysate was followed by pipetting up and down. Then NucleoSpin® RNA XS columns were placed in collection tubes and the lysate was transferred to the columns. For binding RNA to membranes, columns were centrifuged at 11,000 x g for 30 sec. Columns were then transferred to new collection tubes. Membrane desalting was achieved by centrifugation at 11,000 x g for 30 sec subsequent to 100µL of MDB buffer (membrane desalting buffer) addition. Further 25 µL rDNase reaction mixture was added directly on the silica membrane and incubated at RT for 15 min in order to digest DNA. First washing step was performed with 100 µL Buffer RA2 and incubation for 2 min at RT was followed by centrifugation at 11,000 x g for 30 sec. Columns were transferred to new collection tubes and second washing step with 400 µL Bufffer RA3 was performed. Subsequent to the centrifugation at 11,000 x g for 30 sec, supernatant were discarded. Last washing step with 200 µL Bufffer RA3 and centrifugation at 11,000 x g for 2 min was done. Finally columns were transferred to new collection tubes and elution of total RNA was achieved with 15 µL RNase-free H_2O. Then the amount and purity of RNA were monitored with NanoDrop spectrophotometer.

2.11. GENE EXPRESSION PROFILE BY Q-PCR

For each organoid culture group, cDNA synthesis was performed with iScript cDNA Synthesis Kit subsequent to total RNA extraction. Complete reverse transcription reaction mix (20µL) was prepared with 4µl of 5X Reaction mix, 1 µL of iScript™ reverse transcriptase, nuclease free water and extracted RNA templates. Prepared samples were incubated at 25°C for 5 min, 46°C for 20 min, and 95°C for 1 min using a thermal cycler. Then real-time PCR was carried out with synthesized cDNAs using iTaq Universal SYBR Green Supermix (2X) to analyze gene expression profiles of Pt specific markers PTH and CaSR; T-specific marker TPO. Beta-actin was selected as a reference gene for normalization of selected marker expressions. Forward (F) and Reverse (R) primer sequences and expected amplicon lengths of target genes are listed in Table 2.7. Real-time PCR reaction mixture for each primer was prepared as given in Table 2.8. The reaction was conducted with Bio-Rad CFX96 C1000 Touch thermal cycler according cycling temperatures given in the Table 2.9. Data analysis was carried out by comparative Ct method (ΔΔ Ct) and data were expressed as fold change.

Table 2.7. Forward (F) and reverse (R) primer sequences utilized in real-time PCR with expected amplicon lengths

Primers	**Sequence (5'→3')**		**Product Length (bp)**
PTH	F	GACATTGTATGTGAAGATGATACC	191
	R	GCTTCTTACGCAGCCATTCTA	
CaSR	F	GGACAGCGGGAACAGGATTTGAGAG	211
	R	CCCAGTTAGTCCCGGTTCCTTCACC	
Beta-actin	F	TGATCCACATCTGCTGGAAGGT	142
	R	GACAGGATGCAGAAGGAGATTACT	

Table 2.8. Real-Time PCR Reaction Set Up

Components	**Volume**
iTaq Universal SYBR Green Supermix (2X)	5 µL
Forward Primer (10 picomol/µL)	0.25 µL
Reverse Primer (10 picomol/µL)	0.25 µL
Template DNA	3µL
Water, nuclease-free	1.5µL
Total Volume	**10 µL**

Table 2.9. Thermal cycling protocol of qPCR

Step	**Temperature (℃)**	**Time**	**Number of Cycles**
Polymerase Activation and DNA Denaturation	95	30 sec	1
Denaturation	95	5 sec	40
Annealing	56	30 sec	
Extension	72	5 min	

After Real-Time PCR was conducted, 2 percent agarose gel was prepared with 1X TBE buffer. For each PCR product, 2 µL of loading dye was added and PCR products were loaded. Agarose gel electrophoresis was performed at 110 V for 60 min. Visualization of result was performed with Biorad Chemidoc XRS device.

3. RESULTS

3.1. CHARACTERIZATION OF ISOLATED CELLS

Morphology of the primary human Pt and T cells in monolayer culture were investigated for cell characterization. Bright-Field (BF) cell culture imaging of isolated Pt and T cells was performed.

Pt cells in monolayer culture demonstrated polygonal shape with spherical nuclei. They have more standardized dimensions with a rather regular shape when compared to T cells (Figure 3.1.a). Pt cell characterization was further supported in terms of biochemical analysis. PTH present in culture medium was measured above 5,000 pg/mL. Immunocytochemical staning performed for further cellular morphology assessment were consistent with these results (Figure 3.2.a-d). Cells exhibited positive staining for membrane protein markers, CaSR and PTHR1. Moreover, cells showed fine granular staining of PTH and Chromogranin A which are biomarkers of secretory chief cells. In light of all these results, Pt cell morphology was confirmed.

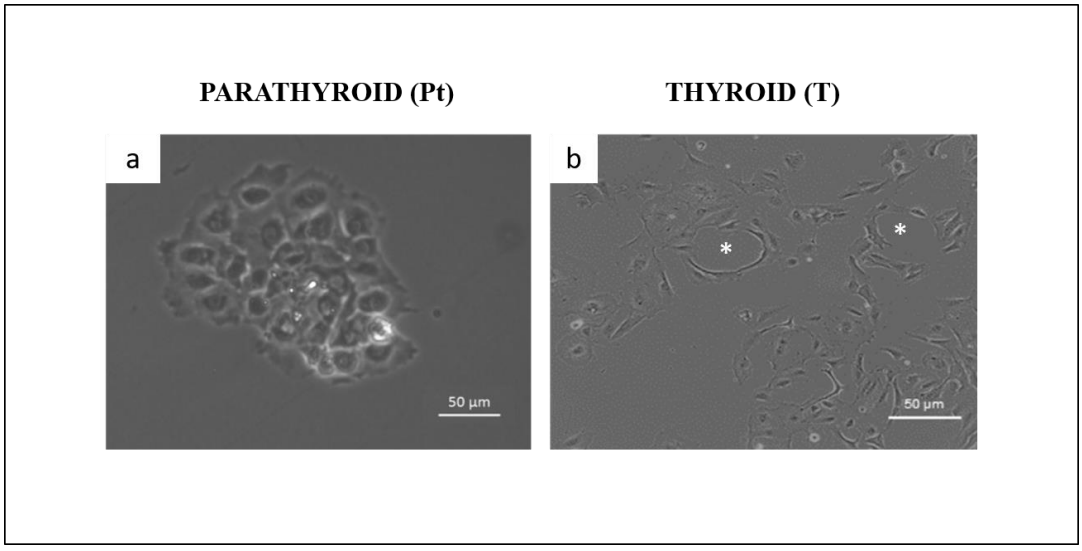

Figure 3.1. Morphological characterization of the primary human parathyroid and thyroid cells individually cultured in their basal mediums. Representative images for (a) Pt and (b) T cells in monolayer culture. Follicular structures indicated with asterisk(*). Scale bars=50 µm

For T cells, fibroblast-like cell morphology was observed by BF imaging. Follicular formations appeared due to the elongated T cells making inner cavities by cell to cell contact. These distinctive structures specific to the T cells represented with asterisk (*) (Figure 3.1.b). These specific functional units of T cells were observed until after the replacement of culture medium from SGM to TGM on day 2. Confirmation of T characterization was also achieved with the immunocytochemical examinations. Cells exhibited positive staining for T specific protein markers which are nuclear protein markers PAX8 and TTF1, membrane protein marker TSHR and internal protein marker FOXE1(Figure 3.3.a-d). Upon red staining of actin filaments, presence of follicular formations also became evident (Fig. 3.3.b,d).

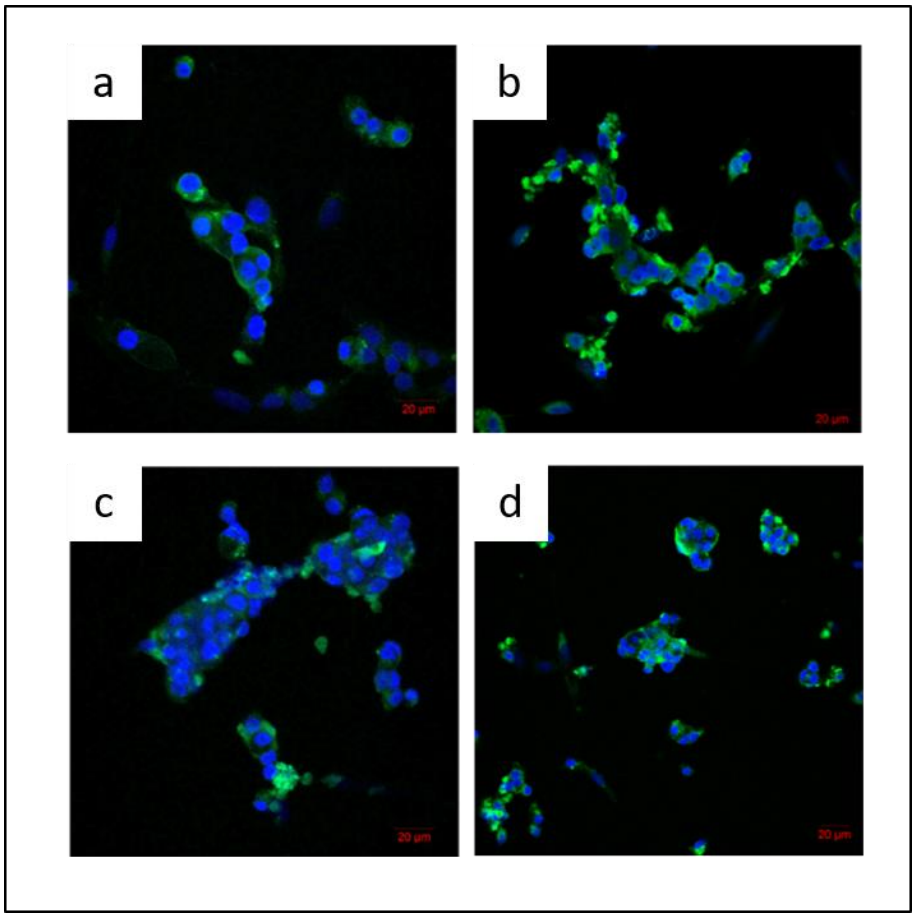

Figure 3.2. Confocal microscopy observations of parathyroid cells after 96 hours of culturing. Representative images for immunofluoresence staining of (a) membrane marker CaSR, (b) internal marker Chromogranin A, (c) internal marker PTH and (d) membrane marker PTHR1 are shown. Staining of whole proteins resulted in green whereas counterstaining of nuclei resulted in blue. Scale bars = 20 μm

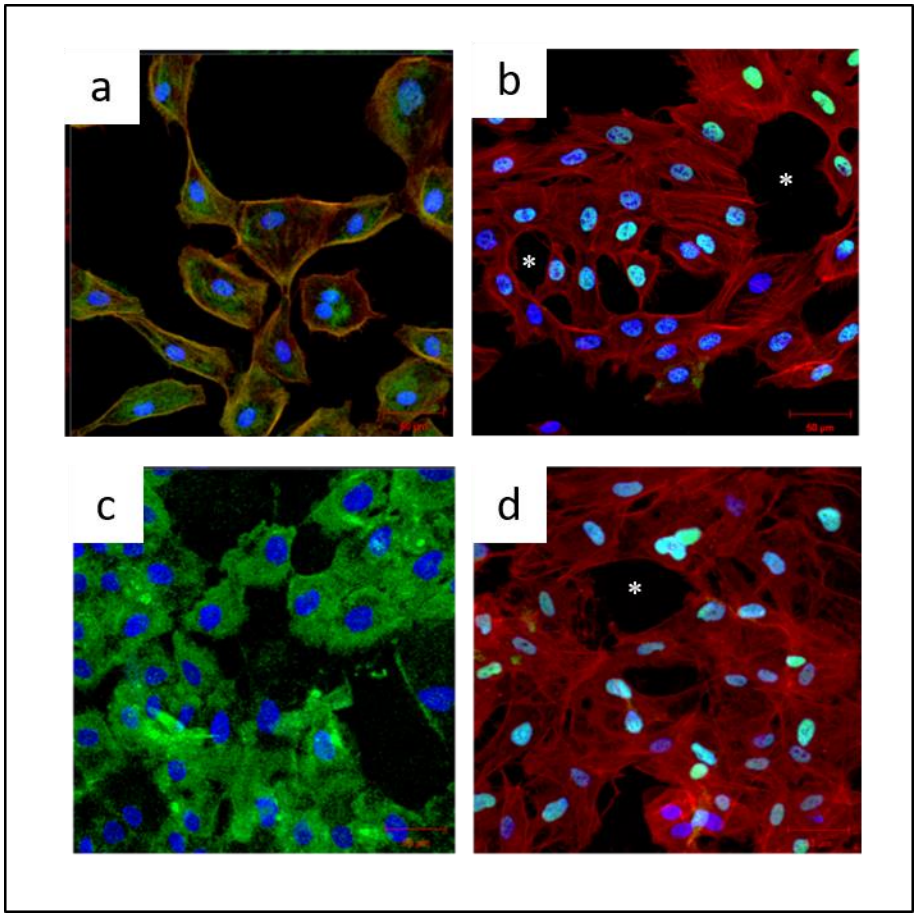

Figure 3.3. Confocal microscopy observations of thyroid cells after 96 hours of culturing. Representative images for immunofluorescence staining of (a) internal marker FOXE1 (b) nuclear marker PAX8, (c) membrane marker TSHR and (d) nuclear marker TTF1 are shown. Staining of whole proteins resulted in green whereas counterstaining of nuclei resulted in blue. Cytoskeleton stained with phalloidin in red in order to observe cellular morphology. Follicular structures indicated with asterisk(*). Scale bars = 50 µm

3.2. CELL LABELING

Following characterization of the isolated T and Pt cells, 3D self-organizing organoids were generated by seeding cells at a density of total 20,000 cells/well into ultra- low attachment 96 well plates. Prior to organoid generation, isolated Pt and Tcells were individually labeled with fluorescent dyes PKH26 (red) and VybrantDiO (green), respectively for the estimation of organizational assembly. Due to lipophilic feature, PKH26 and Vybrant DiO dyes have an ability to bind to the membrane of the cells. Cellular distribution and the 3D architectural features of the COC organoids were evaluated by individually labeled Pt and Tcells with a distinctive fluorescent colors. While the Pt cells appeared in red, T cells appeared in green color under the fluorescent microscopy. Figure 3.4. shows fluorescently labeled organoids generated by only Pt cells and only T cells. Since the structure was not clear in organoids consisting of either Pt or T cells alone, BF images and fluorescent images were overlapped to obtain merged images. Pt organoid culture in PGM had more tightly packed cells all seen in red (Figure 3.4.a) whereas T organoid culture in TGM represented distinctive follicular like morphology (Figure 3.4.b). The unstained oval structures (indicated by asterisks) that were surrounded by fluorescently labeled T cells showed morphology of follicle which is the specific functional unit of T cells.

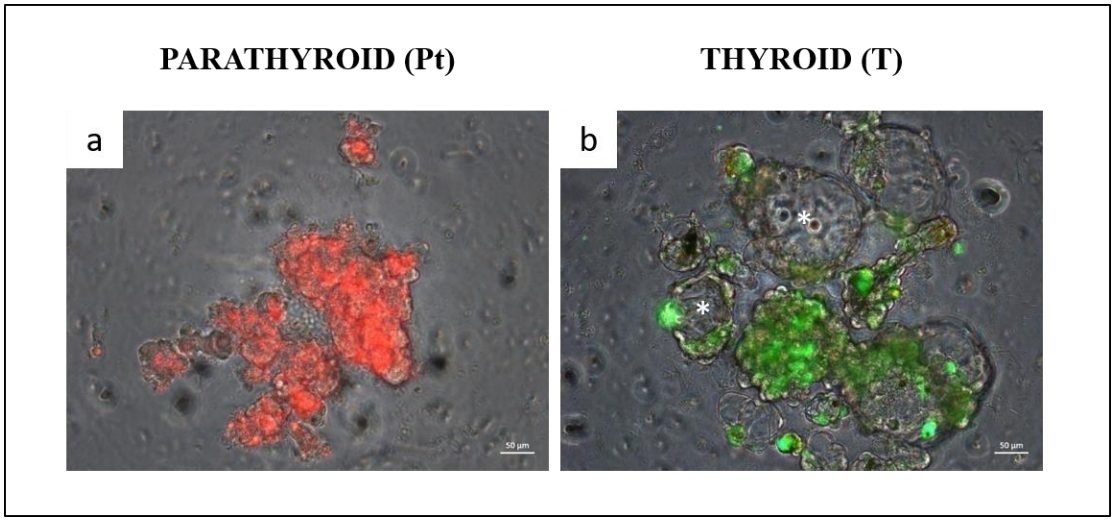

Figure 3.4. Merged fluorescent and bright-field observations of PKH26 (in red)and VybrantDiO (in green) labeled organoids at day 7. Representative images for immunofluorescence staining of (a) Pt in PGM (b) T in TGM. Scale bars = 50 µm

After formation of 3D organoids, COC organoid groups were induced by changing the mediums, from standard growth medium (SGM) to differentiation medium (DM) on day 2. Fluorescent microscopy imaging of the generated organoids were done on days 2, 7 and 14 (Figure 3.5.).

Bright Field microscopy observations of COC organoids were also obtained to better elucidate changes in size and morphology of organoids over time (Figure 3.6.). As T and Pt cells were combined to generate COC organoids, each group represented heterogenic morphologic features belonging to T and Pt. The follicular like structure of the generated COC organoids became visible only by day 7. Also this structure was observed more obviously after 14 days of incubation. Since the 1:16 (Pt:T) organoid group contained the highest proportion of T cells, this structure was much more prominent when compared to the other groups (Figure 3.5.n,o and Figure 3.6.n,o). According to the microscopic observations, the increase in T cell proportion within the generated COC organoid groups also resulted in an increase in the observed green labelled cell presence (Figure 3.5.). When the results of the 2nd day and 7th day were compared, it was observed that the relatively smaller and scattered cellular clusters came together to form larger organoid structures (Figure 3.5.a,b,d,e,g,h,j,k,m,n). Considering organoid morphologies on day 2, Pt cells (red) were mostly observed in the inner parts and T cells (green) appeared in the outer (Figure

3.5.a,d,g,j,m). However, in general, Pt cells did not show specific localization or organizational assembly in cultured organoids. However both on day 7 and 14, T cells shown in green tended to be localized more in the peripheral region whereas Pt cells shown in red tended to be mainly in the central region (Figure 3.5.c,f,i,l,o).

The average diameter of COC organoids were quantified ranging from 439 μm to 658 μm at days 2, 7 and 14 (Figure3.7.). After 14 days of incubation, COC organoids generated using a lower amount of thyroid (COC 1:1 (Pt:T) and COC 1:2 (Pt:T)) were mostly observed as smaller structures. In organoids, with the exception of COC 1:2 (Pt:T), increased T cell amount in organoids also resulted in an increase in the size of the cultures. The largest organoid sizes were observed with the COC 1:16 (Pt:T) organoids on day 14. COC 1:16 (Pt:T) showed the most dramatic increase in diameter at day 14 and were 36 percent larger at this time point compared to day 2. Two way ANOVA was performed to compare the significant differences in the average diameters between day 2 versus day 7, and day 2 versus day 14. Statistically significant increases in the diameter of COC 1:4 (Pt:T) with p value < 0.05 and COC 1:16 (Pt:T) with $p < 0.001$ were observed at the end of day 14. When COC sizes of the samples between day 2 and day 7 were compared, only the COC 1:2 (Pt:T) showed a significant increase, however organoids became smaller after day 7.

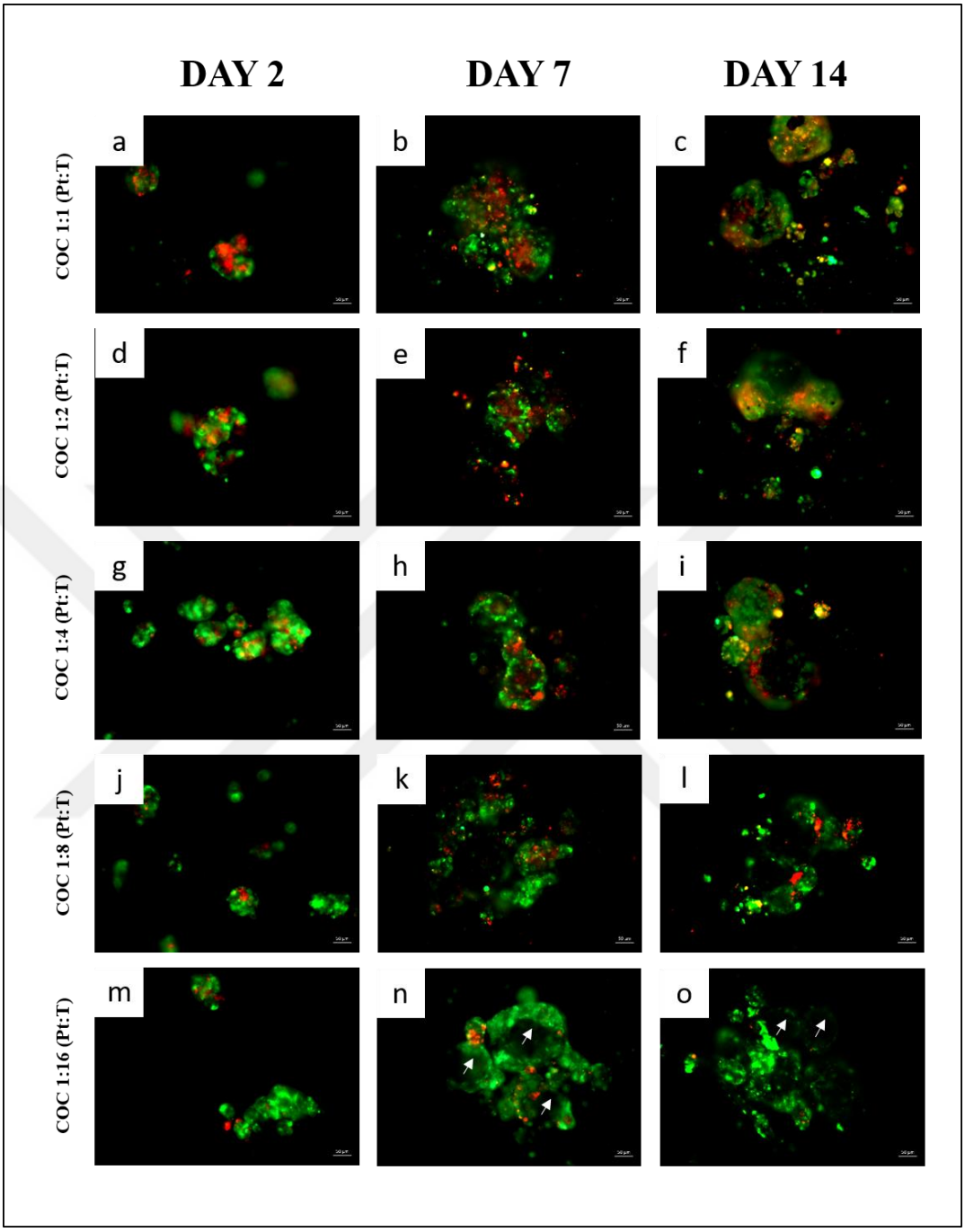

Figure 3.5. Fluorescent microscopy observations of COC organoids in which Pt cells were labeled with PKH26 (in red) and T cells were labeled with VybrantDiO (in green). Representative images for immunofluorescence staining of (a,b,c) COC 1:1 (Pt:T), (d,e,f) COC 1:2 (Pt:T), (g,h,i) COC 1:4 (Pt:T), (j,k,l) COC 1:8 (Pt:T), (m,n,o) COC 1:16 (Pt:T) organoids in DM on days 2,7, and 14. Follicular structures indicated with arrows. Scale bars = 50 μm

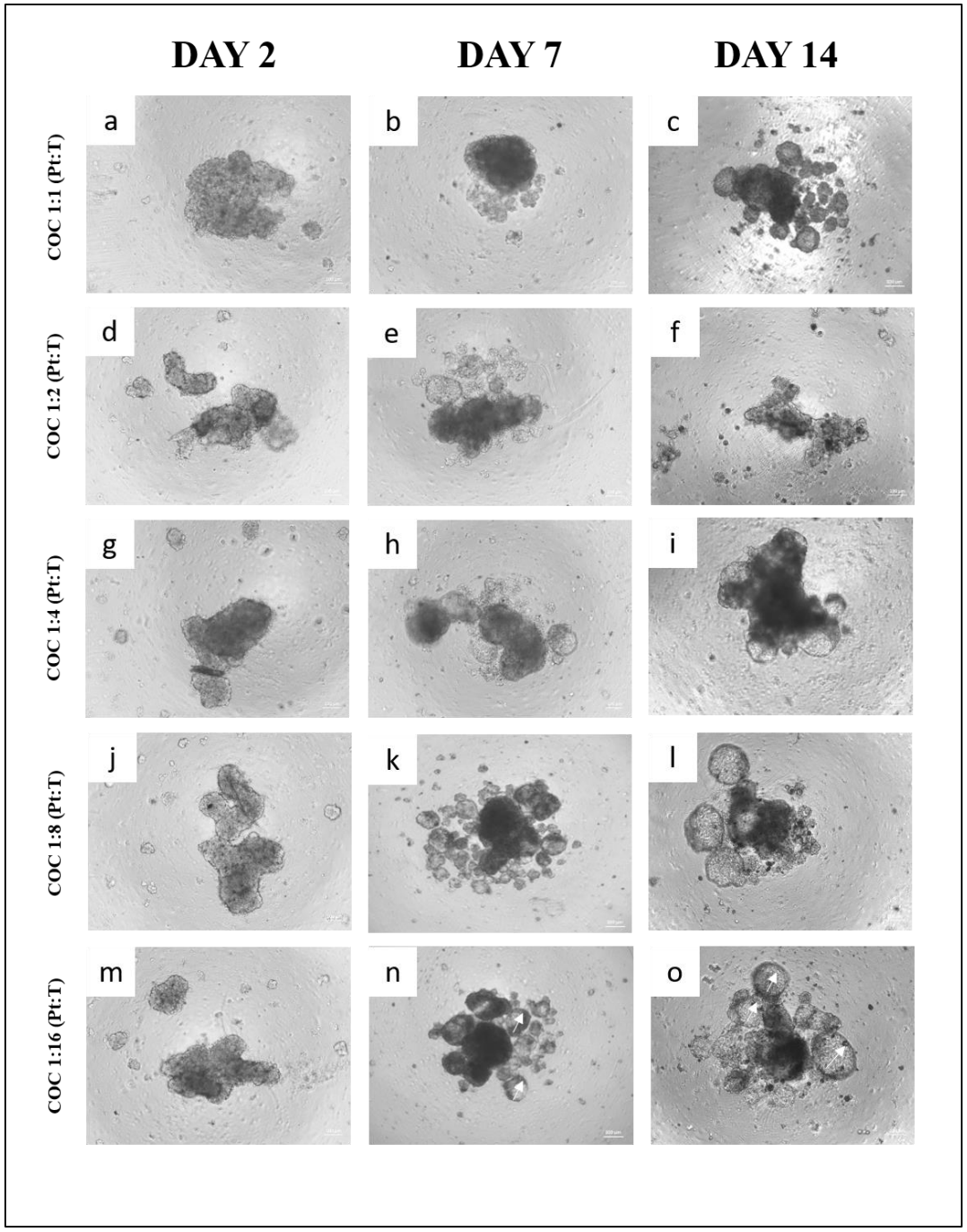

Figure 3.6. Bright Field microscopy observations of COC organoids. Representative images for (a,b,c) COC 1:1(Pt:T), (d,e,f) COC 1:2 (Pt:T), (g,h,i) COC 1:4 (Pt:T), (j,k,l) COC 1:8 (Pt:T), (m,n,o) COC 1:16 (Pt:T) organoids in DM on days 2,7, and14. Follicular structures indicated with arrows. Scale bars = 100 μm

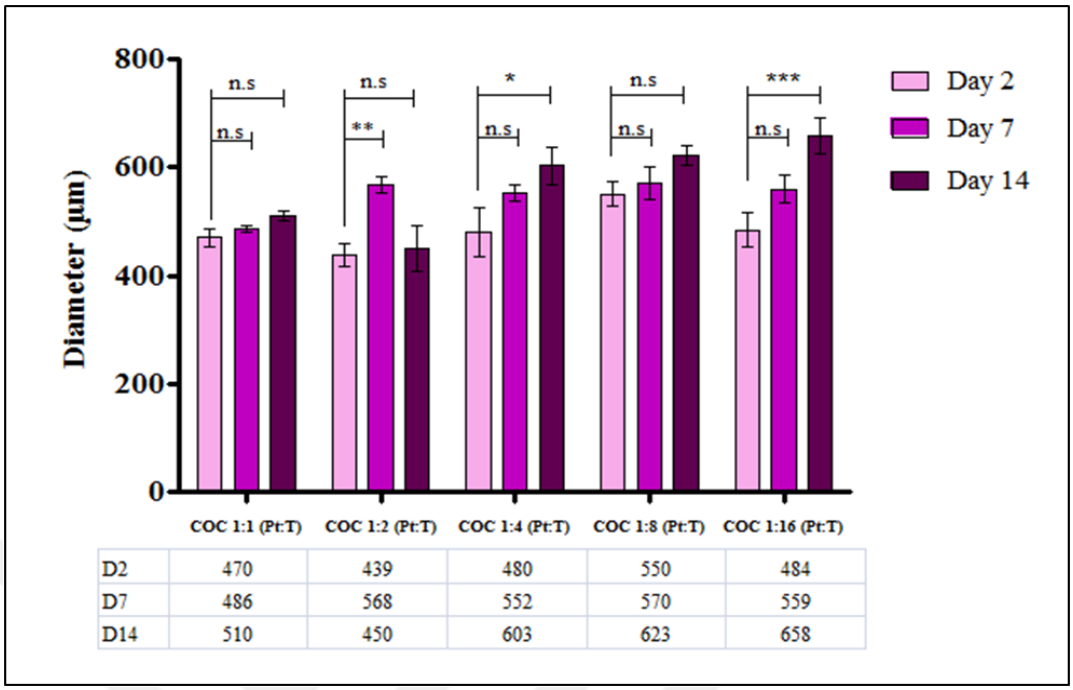

D2	470	439	480	550	484
D7	486	568	552	570	559
D14	510	450	603	623	658

Figure 3.7.Average organoid diameters (n=4, µm) of each COC group after 2, 7 and 14 days of incubation. Two way ANOVA was used to compare the significant differences ($p<0.05$) in the cell diameter change between day 2 versus day 7, and day 2 versus day 14. Error bars indicate standard deviation. *p< 0.05, **p< 0.01, ***p< 0.001, n.s is not significant

3.3. LIVE/DEAD VIABILITY ASSAY

Viability of the generated organoids was evaluated by Live/Dead assay on day 7 and day 14. Live cells were indicated with Calcein-AM stain (green) and dead cells were indicated with Ethidium homodimer-1(red) (Figure3.8.). Results demonstrated that in all organoid cultures, over 90 percent viability was observed. Dead cells incorporated with Ethidium homodimer-1 were distinguished in red and visualized most particularly along the edges of the spheroids.

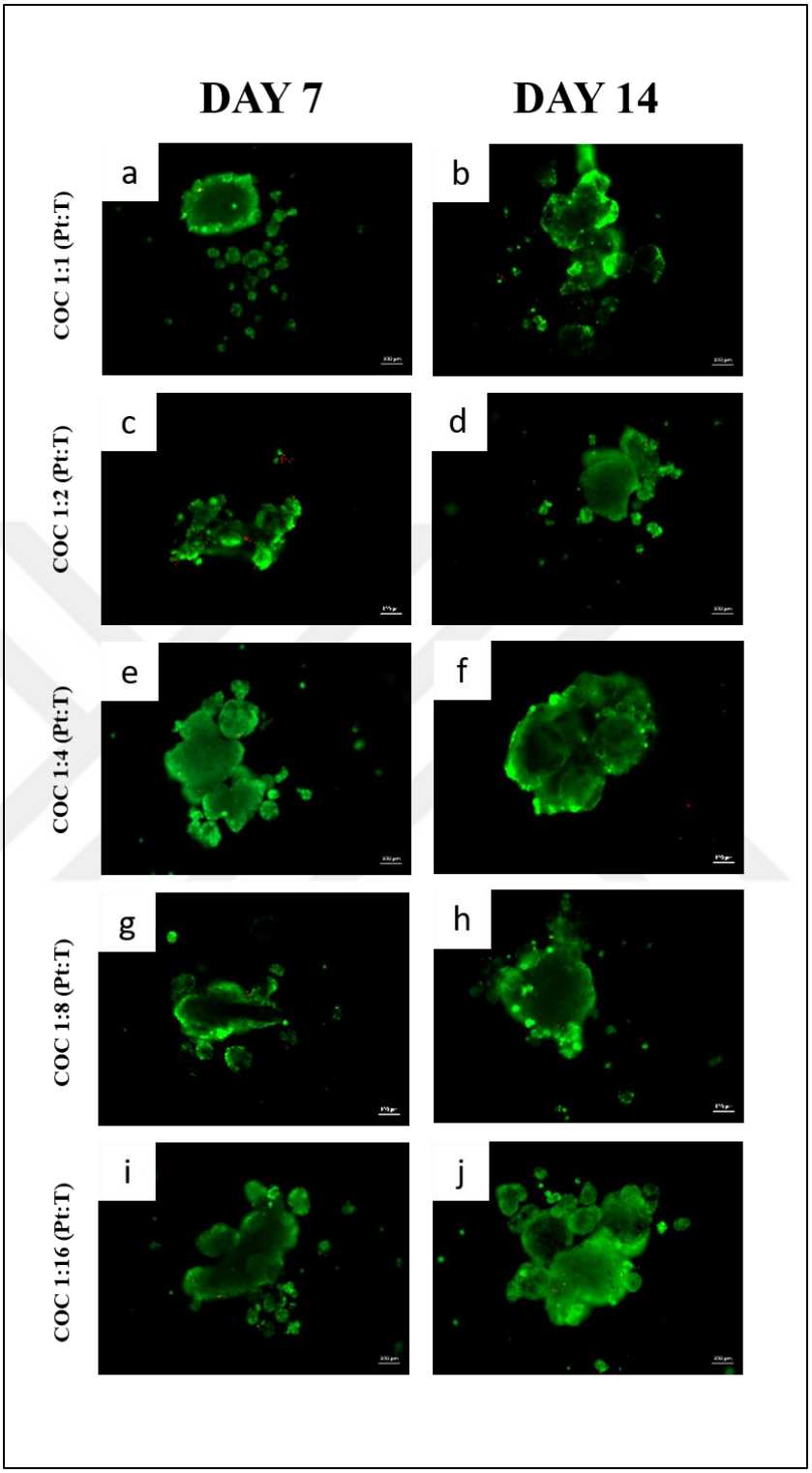

Figure 3.8. Live/Dead Viability Assay with fluorescent microscope imaging. Representative images of organoids stained with Calcein-AM (green) and Ethidium homodimer-1 (red) on days 7 and 14. Scale bars=100 μm

3.4. IMMUNOHISTOCHEMICAL ANALYSIS

The immunohistochemical profile of the paraffin sectioned organoids were observed under the microscope (Figures 3.9., 3.10. and 3.11.). Unfortunately, not enough specimen sections were obtained for IHC from all COC organoid groups. IHC analysis of only COC 1:1 (Pt:T), COC 1:4 (Pt:T) and COC 1:16 (Pt:T) organoids was performed. Firstly, the paraffin embedded parathyroid (Pt), thyroid (T), COC 1:1 (Pt:T), COC 1:4 (Pt:T) and COC 1:16 (Pt:T) organoid sections were stained with haematoxylin and eosin (Figure 3.9.). Pt organoid (Figure 3.9.a), was different from T organoid (Figure 3.9.b) and COC organoids (Figure 3.9.c,d,e) in terms of cell structure. In Pt organoid, cells having small round nuclei with partially clear/vacuolated cytoplasm that were tightly attached to each other were detected. In the T and COC organoids, on the other hand, cells with larger eosinophilic cytoplasm were observed. More loosely assembled cells were observed in these organoids, which occasionally resulted in the formation of slit-shaped spaces/cavities. These clearly visible cavities were thyroid-specific follicle structures and the occurence of follicles was much more prevalent in COC organoids having a higher proportion of thyroid cells; COC 1:16 (Pt:T), COC 1:4 (Pt:T) and COC 1:1 (Pt:T) in descending order. In COC 1:1 (Pt:T), most of the cells were small cells with round nuclei with eosinophilic cytoplasm (Figure 3.9.c). In addition, larger cells with clear cytoplasm with nuclei pushed aside were also seen. However, in this example there was no appearance of cells coming together to form gaps in the middle as in COC 1:16 (Pt:T) (Figure 3.9.e). In other words, the follicle structure could not be observed clear enough due to decreased amount of T usage in organoid construction. IHC results showed the co-existence of Pt and T cells in COC organoids.

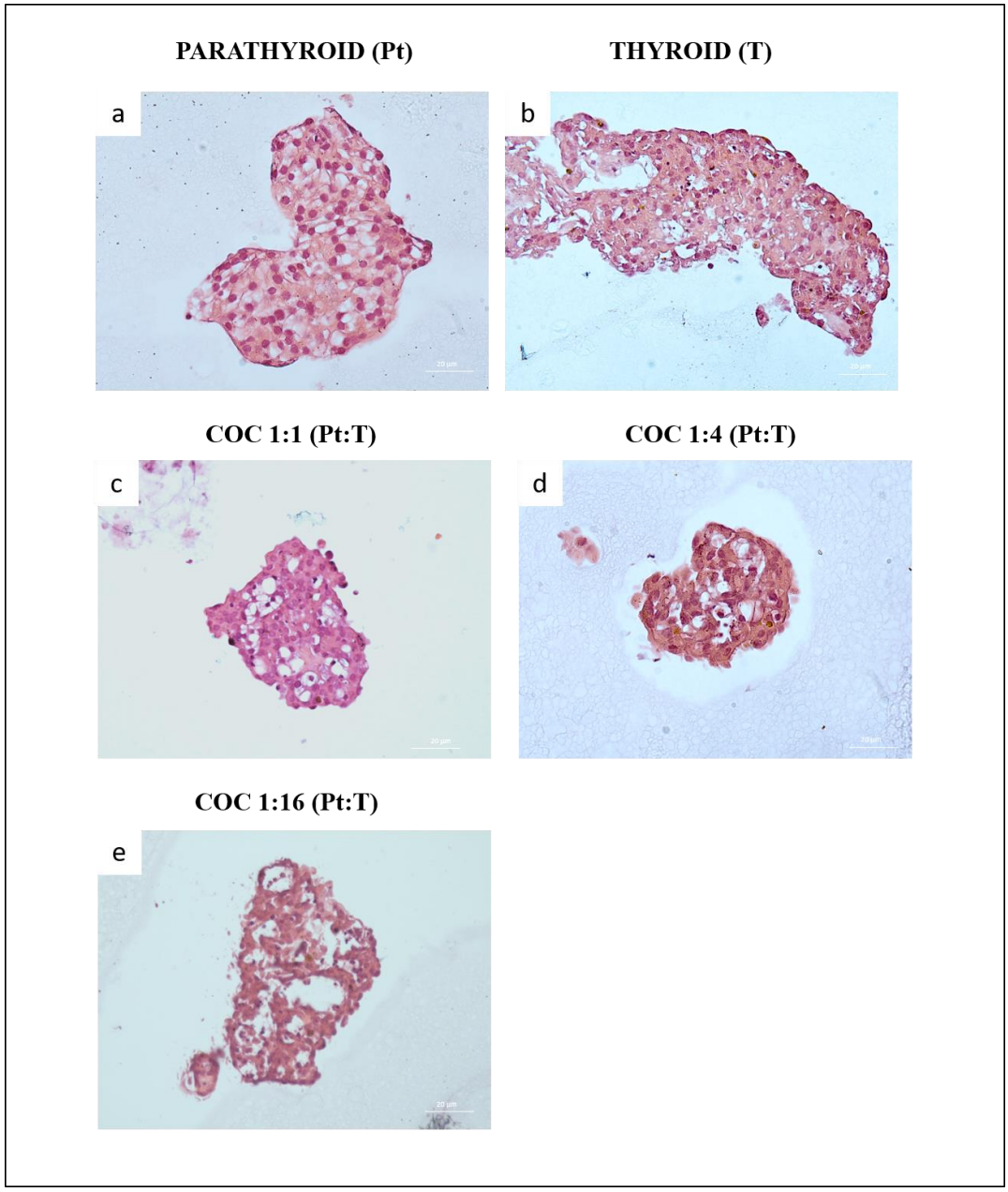

Figure 3.9. Hematoxylin-Eosin staining of organoids. Representative images for (a) Pt, (b) T and (c) COC 1:1 (Pt:T), (d) COC 1:4 (Pt:T),and (e) COC 1:16 (Pt:T) organoids after 14 days of incubation in PGM, TGM and DM, respectively. Scale bars = 20 µm

For further IHC characterization, COC organoids were stained with TTF1 as T specific nuclear marker and with PTH and CaSR as Pt specific membranous cytoplasmic markers (Figures 3.10. and 3.11.). Cross-sections cannot be taken from all COC organoids, the IHC results of organoids COC 1:1 (Pt:T), COC 1:4 (Pt:T) and COC 1:16 (Pt:T) were shown in Figure 3.10. and Figure 3.11. The positive control groups, was shown together with COC 1:1 (Pt:T), in Figure 3.10. Pt tissue sections were used as a positive control of PTH staining and cytoplasmic brown staining was observed in all Pt cells (Figure 3.10.a). T tissue sections were used as a positive control of nuclear brown TTF1 staining (Figure 3.10.c). In the COC 1:1 (Pt:T) sample, it was observed that small cells with round nuclei with eosinophilic cytoplasm were TTF1 positive, while cells with clear cytoplasm were observed as TTF1 negative (Figure 3.10.d). Unlike TTF1, small cells with round nuclei with eosinophilic cytoplasm were negative with respect to PTH, while cells with clear cytoplasm were PTH positive (Figure3.10.b). COC 1:4 (Pt:T) organoids demonstrated positive PTH staining in some regions (Figure 3.11.a). Cytoplasmic brown staining that indicates presence of Pt cells were especially observed in the centre of COC 1:4 (Pt:T) organoids. On the other hand, small cells with round nuclei with eosinophilic cytoplasm appearing positively stained with TTF1 were observed in the peripheral rather than the centre of the organoid (Figure 3.11.c). Moreover, cells with clear cytoplasm were TTF1 negative. According to IHC results, Pt cells were mostly surrounded by peripherally localized T cells, which is consistent with cell labeling results. Additionally, COC 1:4 (Pt:T) organoids demonstrated positive staining of CaSR which is the principal PTH secretion regulator (Figure 3.11e). Taken these results together, in COC 1:4 (Pt:T) organoids, presence of Pt and T cells were confirmed immunohistochemically. Also similar to COC 1:1 (Pt:T), small cells with round nuclei with eosinophilic cytoplasm were negative with respect to PTH whereas cells with clear cytoplasm in the focal areas were PTH positive in COC 1:16 (Pt:T) (Figure 3.11b). The PTH positivity was observed in COC 1:1 (Pt:T) more than the one in COC 1:16 (Pt:T) sample due to the excess amount of Pt cell use in organoid production. However, despite the increase in the amount of T cells, there was no prominent increase in TTF1 positivity (Figure 3.11d). Furthermore, COC 1:16 (Pt:T) organoids demonstrated positive staining of CaSR that is the principal PTH secretion regulator like COC 1:1 (Pt:T) and both COC 1:4 (Pt:T) (Figure 3.11.f).

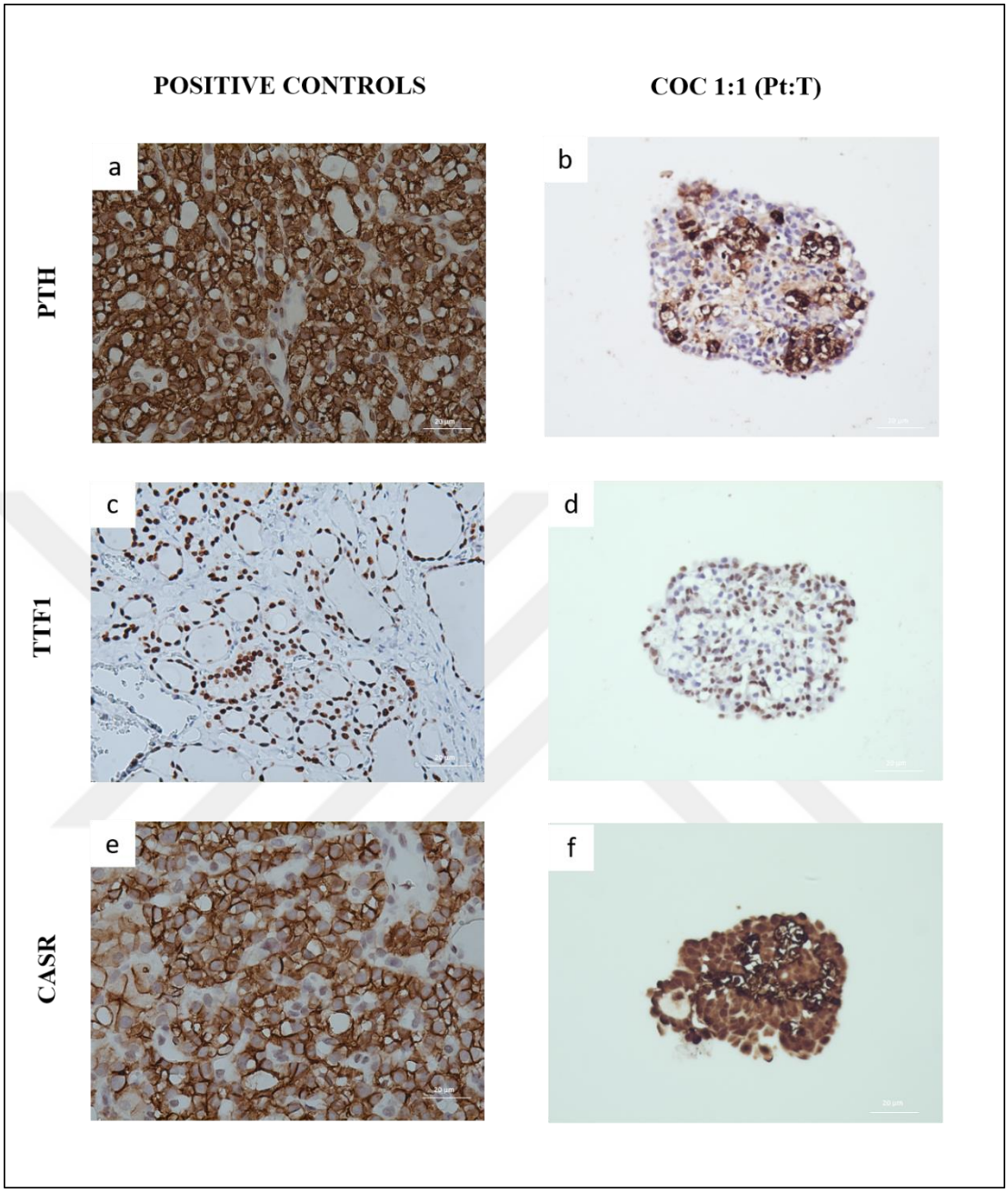

Figure 3.10. IHC analysis of COC 1:1 (Pt:T) organoids after 14 days of incubation in DM. Representative images for PTH staining of (a) positive control, and (b) COC 1:1 (Pt:T) organoid; TTF1 staining of (c) positive control, and (d) COC 1:1 (Pt:T) organoid; CaSR staining of (e) positive control and (f) COC 1:1 (Pt:T) organoid. Scale bars = 20 µm

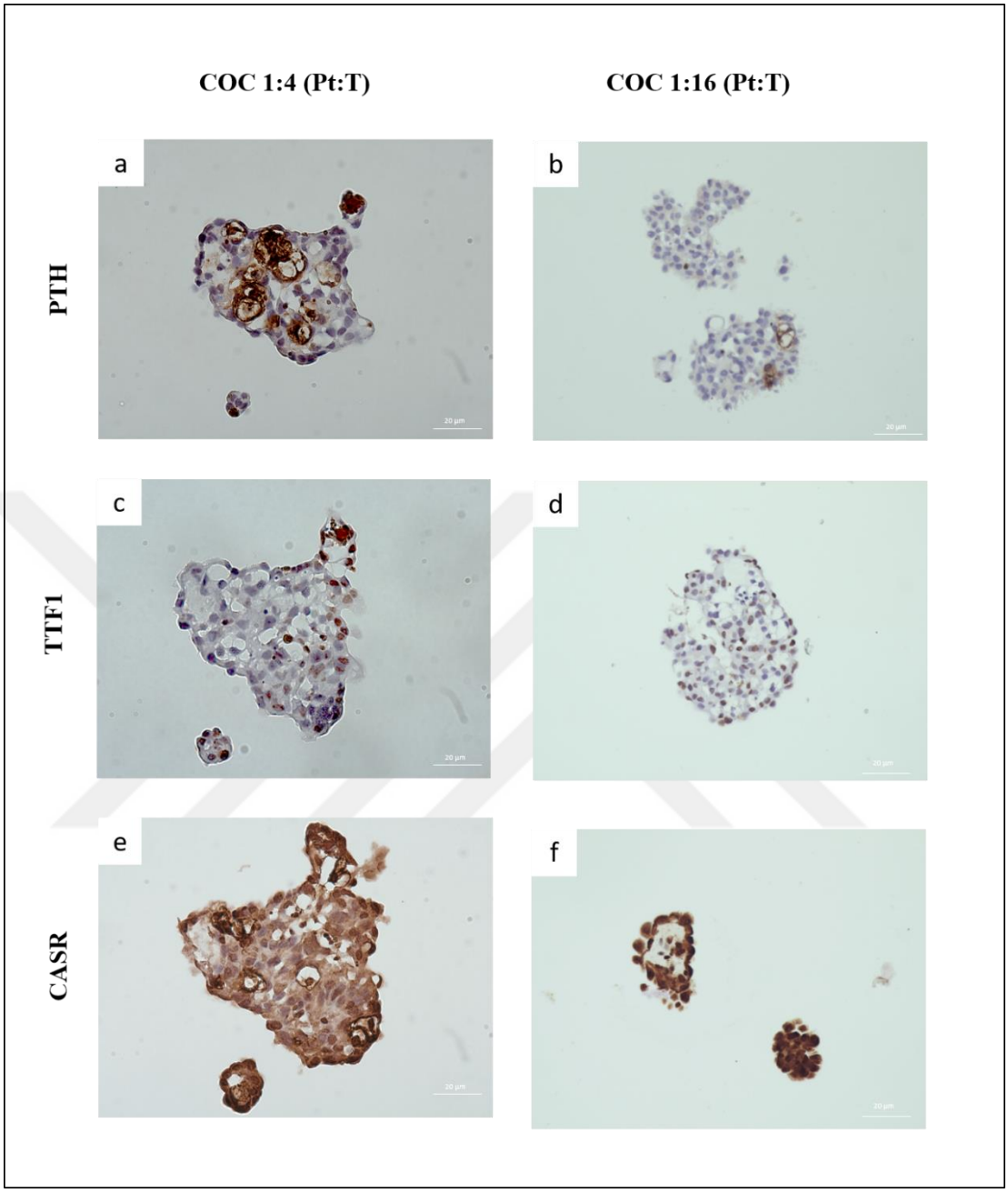

Figure 3.11. IHC analysis of COC 1:4 (Pt:T) and COC 1:16 (Pt:T) organoids after 14 days of incubation in DM. Representative images for PTH staining of (a) COC 1:4 (Pt:T),and (b) COC 1:16 (Pt:T); TTF1 staining of (c) COC 1:4 (Pt:T), and (d) COC 1:16 (Pt:T); CaSR staining of (e) COC 1:4 (Pt:T) and (f) COC 1:16 (Pt:T) organoid. Scale bars = 20 µm

Due to the problems experienced in sectioning, only PTH staining of Pt organoid could be possible apart from H&E staining. Cytoplasmic brown staining indicating the PTH positivity was not observed in Pt organoid's all cells although it was composed of only Pt cells (Figure 3.12.).

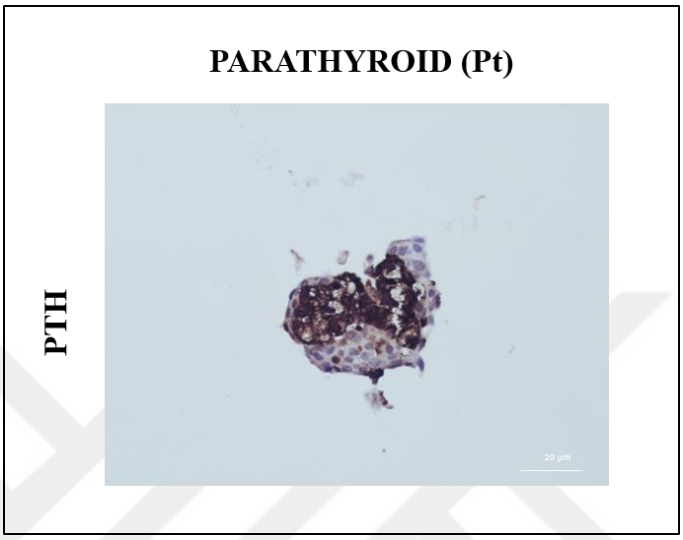

Figure 3.12. IHC analysis of Pt organoid after 14 days of incubation in PGM. Representative image for PTH staining of Pt organoid. Scale bars = 20 μm

3.5. BIOCHEMICAL ANALYSIS

Functionality of the generated organoids with varying concentrations of Pt to T cells were evaluated biochemically with PTH measurement. For the biochemical confirmation of PTH secretion, ELISA was performed on the culture medium of each organoid group at the end of 2, 7 and 14 days of incubation. Pt and T organoids were grown in their basal media, PGM and TGM, respectively, throughout 14 days of incubation period. COC organoids were first seeded in SGM and transferred to DM after day 2 to trigger differentiation. Hence specific media (TGM, PGM, SGM, DM) at specific time intervals were used for blank subtraction in measuring PTH secretion.

Table 3.1. and Figure 3.13. present the PTH measurement results for 14 days of incubation period with determined time intervals. While PTH secretion was measured above 5,000 pg/mL for the Pt organoid in PGM at all time points, no secretion was observed in the T organoid in TGM. All the COC organoid groups show gradual increase in PTH secretion

after the induction with conditioned media as DM. When the PTH measurements of D7 and D14 was compared with the D2 within each group, the greatest increase in PTH secretion was observed in COC 1:16 (Pt:T). Besides closer inspection of the results shows that COC 1:16 (Pt:T) has the lowest PTH secretion when compared to other COC groups due to the decreased total thyroid cell number usage in organoid formation (Figure 3.13.). Taken together, these results suggest that the increase in PTH secretion is highest for COC 1:16 even though Pt to T proportion used in organoid formation is reduced.

The increase in PTH secretions on the 7th and 14th days were calculated for each group as a percentage by making comparison with 2nd day values. According to Table 3.1., D7 results indicate that secretion increased by 41 percent for COC 1:1 (Pt:T) , 202.8 percent for COC 1:2 (Pt:T), 475.8 percent for COC 1:4 (Pt:T), 374.2 percent for COC 1:8 (Pt:T) and 647.9 percent for COC 1:16 (Pt:T). D14 results indicate that secretion increased by 559.5 percent for COC 1:4 (Pt:T), 1725 percent for COC 1:8 (Pt:T) and 728.7 percent for COC 1:16 (Pt:T). When COC groups were compared with each other, it is seen that PTH secretion was measured above 5000 pg/mL on D14 for COC 1:1 (Pt:T) and COC 1:2 (Pt:T) just like the Pt organoid. Also PTH secretion result of COC 1:4 (Pt:T) organoid group approaches this value with 4531 pg/mL secretion. As seen in Figure 3.13., statistically significant ($p<0.001$) increases in PTH release observed between day 2 versus day 7, and day 2 versus day 14 for all COC organoids (two way ANOVA).

Table 3.1. PTH measurement results (pg/mL) of generated organoids at days 2, 7 and 14

	T	**Pt**	**COC 1:1 (Pt:T)**	**COC 1:2 (Pt:T)**	**COC 1:4 (Pt:T)**	**COC 1:8 (Pt:T)**	**COC 1:16 (Pt:T)**
D2	0	>5,000	2,317	1,334	687	392	167
D7	0	>5,000	3,267 (+ % 41)	4,040 (+ % 202.8)	3,956 (+ % 475.8)	1,859 (+ % 374.2)	1,249 (+ % 647.9)
D14	0	>5,000	>5,000	>5,000	4,531 (+ % 559.5)	1,725 (+ % 340)	1,384 (+ % 728.7)

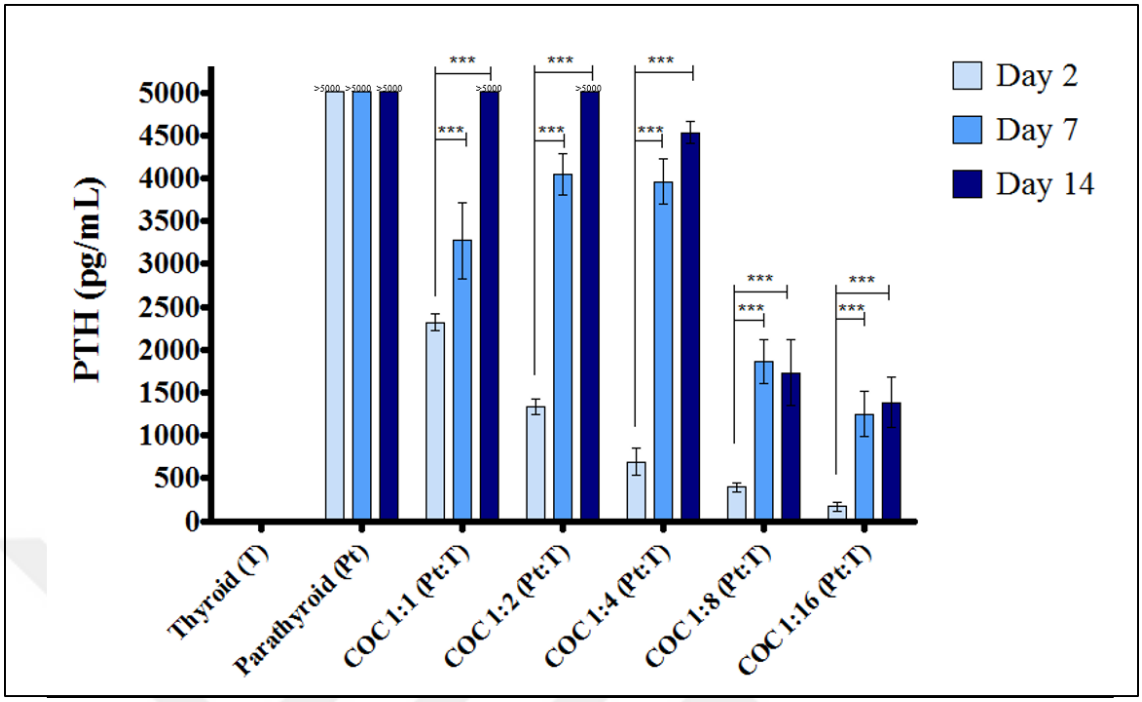

Figure 3.13. PTH secretion (pg/mL) from the Thyroid(T), Parathyroid (Pt) and COC organoids on days 2,7 and 14. For Pt on D2,7 and 14 along with COC 1:1(Pt:T) and COC 1:2 (Pt:T); PTH release results above 5,000 pg/mL are represented by > 5,000. Two way ANOVA was used to compare the significant differences ($p<0.05$) between day 2 versus day 7, and day 2 versus day 14. Error bars indicate standard deviation. *p< 0.05, **p< 0.01, ***p< 0.001, n.s is not significant

Measured PTH release values were divided by the amount of seeded Pt cells while forming organoids for each COC group and computational normalization was performed. Here, it was aimed to observe the effect of the amount of Pt cells on hormonal secretion comparatively. In Table 3.2, PTH release per Pt cell in COC groups on days 2,7, and 14 is presented. PTH release per Pt cell at both D7 and D14 was observed from the highest to the lowest as follows: COC 1:16 (Pt:T), COC 1:4 (Pt:T), COC 1:8 (Pt:T), COC 1:2 (Pt:T), COC 1:1 (Pt:T). According to the calculations, it was expected to obtain values close to each other in the amount of PTH produced per cell. However, as can be seen in D7, these values varied between 0.326 and 1.06 pg/mL. If only parathyroid cells secreted PTH, the PTH per cell measured results should be nearly equal, the differences in between groups were due to the differentiated T cells.

Table 3.2. PTH release per Pt cell in COC groups (pg/mL) on days 2, 7 and 14

	COC 1:1 (Pt:T)	**COC 1:2 (Pt:T)**	**COC 1:4 (Pt:T)**	**COC 1:8 (Pt:T)**	**COC 1:16 (Pt:T)**
Number of Pt cells used in organoid construction	10,000	6,666	4,000	2,222	1,176
PTH Release per Pt cell on D2	0.2317	0.2001	0.171	0.176	0.142
PTH Release per Pt cell on D7	0.327	0.606	0.989	0.836	1.06
PTH Release per Pt cell on D14	>0.50	>0.75	>1,132	0.776	1.176

Since the group with the lowest amount of PTH produced per cell on day 7 was the COC 1:1 (Pt:T) group containing the highest Pt cell in organoid formation, computational normalization was performed using the values of this group. The expected PTH release amounts for the other COC groups were obtained by multiplying the number of Pt cells used in the organoid structure for each group by COC 1:1 (Pt:T) value of PTH release per Pt cell for the relevant day (Table 3.3.). The differentiation of the T cells into Pt cells was evaluated by comparing Table 3.1., which shows the measured PTH release values, and Table 3.3., which shows the expected PTH release values as a result of the calculation. When the Table 3.1 and Table 3.3. are examined, it can be seen that D7 PTH release value of COC 1:2 (Pt:T) organoid was 4,040 pg/mL while expected PTH release value was 2,180 pg/mL. D7 PTH release value of COC 1:4 (Pt:T) organoid was 3,956 pg/mL while expected PTH release value was 1,308 pg/mL. D7 PTH release value of COC 1:8 (Pt:T) organoid was 1,859 pg/mL while expected PTH release value was 727 pg/mL. D7 PTH release value of COC 1:16 (Pt:T) organoid was 1,249 pg/mL while expected PTH release value was 385 pg/mL. On D14, the expected PTH release for COC 1:2 (Pt:T) was calculated over 3,333 pg/mL and for COC 1:4 (Pt:T) it was over 2,000 pg/mL, but actually for both organoid groups over 5,000 pg/mL PTH release was measured. Moreover, D14 PTH release value of COC 1:16 (Pt:T) organoid was 1,384 pg/mL while expected PTH release value was 588 pg/mL. D14 PTH release value of COC 1:8 (Pt:T) organoid was 1,725 pg/mL while expected PTH release value was 1,111 pg/mL. The actual PTH values of each group were measured to be higher than the expected PTH release values.

Table 3.3. Expected PTH release amounts of COC groups (pg/mL) on days 2, 7 and 14. COC 1:1 (Pt:T) organoid was chosen for the normalization as it was constructed with the highest amount of Pt cells

	COC 1:2 (Pt:T)	**COC 1:4 (Pt:T)**	**COC 1:8 (Pt:T)**	**COC 1:16 (Pt:T)**
D2	1,545	927	515	272
D7	2,180	1,308	727	385
D14	>3,333	>2,000	1,111	588

3.6. GENE EXPRESSION PROFILE BY Q-PCR

Gene expression profile of COC organoids were evaluated by qPCR after 14 days of differentiation with DM. Gene expression values were represented as fold change and calculated using $2^{-\Delta\Delta Cq}$ method. As seen in Table 3.4., PTH expression was not observed in T organoid in TGM. The highest PTH expression (25.6 fold) was observed in Pt organoid and the least PTH expression was observed in COC 1:16 (Pt:T) organoids. The expression of PTH can be listed in descending order as COC 1:1 (Pt:T), COC 1:8 (Pt:T), COC 1:4 (Pt:T), COC 1:2 (Pt:T) and COC 1:16 (Pt:T). The highest CaSR expression (28.2 fold) was observed in COC 1:4 (Pt:T) organoid and the least CaSR expression was observed in COC 1:8 (Pt:T) organoids. Additionally, the expression of CaSR can be listed in descending order as COC 1:4 (Pt:T), COC 1:2 (Pt:T), T, COC 1:1 (Pt:T), COC 1:1 (Pt:T) and COC 1:8 (Pt:T).

Table 3.4. qPCR results of organoids after 14 day of incubation. The PTH and CaSR gene expression values were represented as fold change and calculated using $2^{-\Delta\Delta C_q}$ method.

Organoid Type	PTH	CaSR
Pt in PGM	25.6	4.3
T in TGM	0.0	6.1
COC 1:1 (Pt:T) in DM	8.8	5.1
COC 1:2 (Pt:T) in DM	6.0	10.9
COC 1:4 (Pt:T) in DM	7.2	28.2
COC 1:8 (Pt:T) in DM	7.6	1.2
COC 1:16 (Pt:T) in DM	4.0	2.4

Furthermore to validate the qPCR results, samples were loaded in 2 percent agarose gel and run at 110V for 60 min. According to the gel electrophoresis results (Figure 3.14.), PTH band was observed in all generated COC organoids but not observed in T organoid. This indicated that functional organoid formation was achieved at the end of 14 days of differentiation application. CaSR band formation was observed faintly in T organoid whereas for COC 1:8 (Pt:T) and COC 1:16 (Pt:T), there was no band formation.

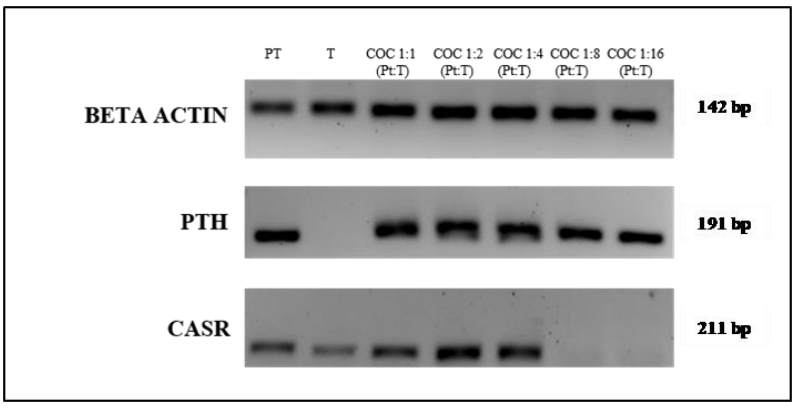

Figure 3.14. Expression of specific markers in COC organoids. Quantitative polymerase chain reaction (qPCR) was performed to detect the expression of PTH, CaSR and reference gene as beta actin

4. DISCUSSION

The main purpose of this study was to create 3D Pt-like organoid structures capable of secreting PTH from stem cells of T tissue in a COC medium for patients with HypoPTH. Considering the close anatomical relationship in adulthood and the common embryonic origin, T cells were selected for COC organoid generation together with Pt cells in this study. To test the hypothesis that stem cells in T tissue can differentiate into Pt-like cells, varying proportions of Pt to T cells were used in formation of COC organoids. Differentiation induction was performed using conditioned medium containing specific growth factors such as Shh and Activin A. *In vitro* evaluations of T to Pt differentiation and organoid functionality were performed in terms of immunohistochemistry, biochemistry and gene expression profile analysis.

In vitro studies with Pt cells date back more than 50 years [69,70]. In the first *in vitro* Pt studies, bovine Pt tissues were used [71,72]. Later studies were carried out with human Pt cells [73]. Pt cells are extremely difficult to culture and thus no Pt cell line establishment protocols were available in the literature until lately [74]. Although there are some reports that achieve culturing Pt cells for long term, short-term culture was used in most of the Pt studies due to their low proliferative activity and high differentiation level [32,75,76]. According to the literature, Pt cells that could be successfully cultured for a long term were usually hyperplastic or adenomatous cells rather than healthy cells. For this reason, hyperplastic human Pt cells were used in this study. However, several studies showed that Pt cells, regardless of being diseased or healthy, may fail to adhere to the culture surface. Furthermore CaSR expression, which is crucial for physiological Pt functionality, can be lost rapidly when cultured as monolayer. Loss of CaSR expression adversely affects the calcium-dependent PTH secretion response of Pt cells [74]. Considering these reasons explained above, researchers attempted to generate 3D formations whose *in vitro* functionality could be preserved by constructing 3D architecture that mimics tissue of origin. In 1986, Ridgeway *et al*. created multicellular aggregates in a monolayer culture system using bovine Pt cells and named them as organoids. With this study, the term Pt organoid was introduced to the literature for the first time [77]. In the following years, another study was conducted with human hyperplastic Pt tissue to construct Pt tissue like architecture. Aggregated human hyperplastic tissue into 3D clusters resulted in long term maintenance of

the Pt cell functionality due to the intercellular contacts [76]. Later, a study investigating the role of cell to cell interactions in the regulation of endocrine secretion showed that PTH release increases when the Pt cells are in closer proximity [78]. Taken together these, organoid construction was performed in this study for better mimicry in functional characteristics of the tissue of origin.

Organoids hold promise for regenerative medicine as disease-causing organs can be replaced by constructing functional biological substitues. They should display similar morphology, 3D structure and functionality with the organ of interest. However, the complexity, large size, and multicellularity of organs in *in vivo* are the key obstacles faced in organoid studies [79]. Additionally, although various organoids including kidney, brain, retina, liver and spinal cord have been successfully developed, their application is limited due to the lack of tissue components such as nerves and blood vessels, which are essential for *in vivo* like organ physiology [80]. Therefore, it is extremely difficult to create an organoid that fully possesses the characteristics of the imitated organ. In the line of these, Pt can be considered as an ideal organoid culture model as being the smallest organ in entire body and exhibiting less complexity compared to the other organs. *In vivo* Pt functionality can be achieved using only chief cells, through PTH secretion [22]. At the same time, the endocrine organs' leaving secretions to the environment instead of a specific duct will ease assessment of Pt organoid functionality [81]. In other words, *in vivo* like Pt functionality can be tested by biochemical evaluation of the samples taken from the culture medium of the generated organoids.

In this study, T cells were cocultured together with Pt cells for 3D Pt-like organoid generation. The main purpose was to differentiate tissue resident stem/progenitor cells in T tissue into Pt-like cells. T cells were chosen as stem cell source due to the close relationship of Pt and T tissues in the embryological period. Both of these endocrine organs differentiate from the third pharyngeal pouch in the embryological period and move inferiorly along the thyroglossal canal. Differentiation continues throughout this movement and eventually the Pt and T organs settle to their natural anatomical locations. When the localization ends, the thyroglossal duct closes [18,22]. Considering this common embryological origin and common embryological movement, T tissue is hypothesized to be a good candidate for stem cell source in Pt differentiation.

Firstly, enzymatic cell isolations were performed from the surgically removed hyperplastic Pt and healthy T tissues to generate COC organoids. Prior to organoid formation, morphological cell characterization of isolated cells was assessed by BF cell culture imaging of individually cultured (monolayer) Pt and T cells in their basal medium. Consistent with the literature, Pt cells demonstrated polygonal shape with spherical nuclei whereas T cells demonstrated rather fibroblast-like morphology [82,83]. In addition, morphological characterization was confirmed by the observation of thyroid-specific functional units called follicles in T cultures [84]. These functional units, seemed to be formed as a result of cell to cell contact of elongated T cells, were observed as prominent structures resembling inner cavities. Also, characterization of Pt cells was further supported in terms of biochemical assays. ELISA test was performed on medium taken from the monolayer cultured Pt cells and PTH release was measured above 5,000 pg/mL.

Afterwards, immunocytochemical investigation of the isolated Pt and T cells was performed by immunofluorescence staining. T cell specific marker proteins as PAX8, TTF1, TSHR and FOXE1 were visualized under fluorescence microscopy. PAX8 was chosen as being a member of lineage specific PAX proteins that are responsible for regulating organogenesis and maintaining the pluripotency of progenitor cells during development. It determines cell fate during thyroid, kidney, brain and eye development [85]. Other T specific marker chosen for immunocytochemical confirmation of T cells is TTF1 which is expressed in the developing T during the embryonic life. TSHR membrane protein marker was chosen as its role in follicular cell differentiation and post-natal growth of T. In addition, T deficiency was observed in FOXE1 knockout mice, so staining was performed with FOXE1 as it was assumed to control the survival of T cells. Monolayer cultured T cells displayed positive staining for all these T-specific protein markers [86]. In addition, red staining of actin filaments with Alexa Fluor™ 647 Phalloidin enabled the morphological observation of the presence of follicular formations in T cells. For Pt characterization, cell specific marker proteins as CaSR, Chromogranin A, PTH and PTH1R were visualized under confocal microscopy. CaSR, a G-protein coupled receptor, is the key regulator of PTH synthesis and secretion for calcium homeostasis maintenance. Therefore, they are mostly expressed in organs involved in calcium metabolism, such as the parathyroid, kidney, and bone [87]. PTH1R which is expressed in most tissues like parathyroid, bone, kidney, ovary, intestine, thymus and liver staining was also investigated [88]. Furthermore, Chromogranin A and

PTH antibody stainings were preferred in Pt cell characterization as they are the key biomarkers of secretory chief cells, which are the functional units of Pt [89]. Since it is difficult to distinguish between Pt and T tissue with naked eye, Pt tissue can sometimes be removed unintentionally by surgeons during thyroidectomy [90]. For this reason, it should be checked whether the isolated T cells are contaminated with Pt cells. Hence morphological, biochemical and immunocytochemical cellular characterization of isolated Pt and T cells was a crucial step before generating organoids.

As the results obtained from immunocytochemistry were in agreement with the morphological characterization results, 3D organoids were generated by seeding Pt and T cells in ultra-low attachment multiwell plates at a constant density of total 20,000 cells per well. To examine the effect of the microenvironment on differentiation and determine the optimal Pt to T ratio required for functional Pt-like organoid formation, COC organoids were generated with varying proportions. In addition to COC (Pt:T) organoids with ratios of 1:1, 1:2, 1:4, 1:8 and 1:16, organoids containing only Pt and only T cells were also created.

Previous studies on Pt-like cell differentiation have used hESC, TEC, TMSC and ADSCs [56,58,60,66]. In these studies, different media formulations were applied for Pt-like cell differentiation. These formulations were mainly derived from renovated version of the D'Amour protocol named Bingham protocol. In general, differentiation formulations contain either Activin A alone or Activin A with varying amounts of Shh. Hence, in this study, all organoids, initially seeded in a SGM, were induced on day 2 with conditioned DM that contains Activin A (100 ng/mL) and Shh (100 ng/mL). It was hypothesized that these specific morphogens enable differentiation of T cells into terminal cell type, Pt-like cells. Activin A, a member of the transforming growth factor-beta (TGF-β) superfamily protein, is a widely used protein that promotes cell differentiation through multiple pathways [91,92]. Shh is a definitive endoderm induction protein that plays crucial roles in cell differentiation during development and maintenance of adult tissues [93].

The purpose of the T cell usage in the study was due to the common embryogenic origin with the Pt as previously mentioned. Furthermore, it was known that both Pt glands, T and thymus are descended from paryngeal endoderm in embryonic development [15]. Thus, the study, which achieved successful differentiation of thymic epithelial cell (TEC) into Pt-like cells with optimized conditioned media, strengthened our hypothesis that there are resident stem cells in the thyroid capable of Pt-like differentiation [58]. In the study with TEC, the

aim was to avoid the alloimmunological barriers associated with hESCs and the potential risk of teratoma formation. Taken all these together, T cells have the similar assets with TECs and chosen to be differentiated into Pt-like cells in this study. Several studies reported that multicellular 3D organoids represents a degree of self-organization that is absent in 2D cultures. To see if this also applies to generated COC (Pt:T) organoids, Pt and T cells were individually stained with distinct lyphophilic surface-labeling fluorescent dyes as PKH26 (red) and VybrantDiO (green), respectively. Labeled cells were then combined into organoids and organoid architecture was evaluated. Morphologic results obtained with fluorescence imaging revealed that Pt cells did not show prominent localization or organizational assembly in COC organoids. However, it seems that T cells tended to be localized at the peripheral zones. Afterwards, the average diameter of COC organoids were measured at days 2, 7 and 14. According to day 14 average diameter results, higher growth in organoid diameter was seen mostly in COC organoids with higher percentage of T cells, although the total cell seeding density (20,000 cells) was kept constant during establishment. Only in COC 1:2 (Pt:T) organoid group, size reduction was observed after day 7. The largest organoid size was observed with COC 1:16 (Pt:T) organoids on day 14. The most dramatic increase (36 percent) in organoid diameter from day 2 to day 14 belonged to COC 1:16 (Pt:T). This result resulted in increased use of T cells in the microenvironment, resulting in larger Pt-like organoids in size. Conversely, biochemical results at day 14 in which the Pt-like functionality of COC organoids were evaluated showed lower PTH release from organoids with a higher amount of T cells. According to ELISA experiment, Pt, COC 1:1 (Pt:T) and COC 1:2 (Pt:T) organoids had the highest PTH release which was measured to be greater than 5,000 pg/mL. These PTH release measurements results were followed by COC 1:4 (Pt:T), COC 1:8 (Pt:T), COC 1:16 (Pt:T) in descending order. Because of the higher percentage of T use in the organoid establishment, lower PTH release was already expected in samples with less T than those with more Pt. However, biochemistry data revealed that organoids containing the least number of Pt cells (COC 1:16 (Pt:T)) had the greatest increase (percent 728.7) in PTH release from day 2 to day 14. This result confirmed the hypothesis that T cells show Pt-like properties after application of DM. In addition, the fact that all generated organoids showed highly significant ($p < 0.001$) increases in PTH secretion at day 14 strengthened this confirmation. Also computational normalization was performed to compare expected PTH release with measured PTH release for each COC organoid and to observe the effect of the amount of Pt cells on hormonal secretion comparatively. The actual

PTH values of each group were measured to be higher than the expected PTH release values for all COC organoids. The difference in between the actual PTH values and expected PTH values was predicted to come from the differentiated T cells. Taken all these biochemistry results together it was demonstrated that T cells were successfully differentiated into Pt-like cells.

In the immunohistochemical analysis, three specific markers, TTF1, PTH and CaSR, were used for T and Pt cells. TTF1 is a protein that regulates the transcription of T cell-associated genes and is used to distinguish T from Pt [94,95]. PTH is specific to Pt chief cells, whereas CaSR is the principal PTH secretion regulator [96,97]. According to the results of IHC characterization of the COC samples, which were successfully sectioned, all three markers showed positive staining. The TTF1 positive cells were mostly in the peripheral zone of organoids, and PTH positive cells were mostly localized in the center. These data obtained were consistent with the cell labeling results. The fact that TTF1 positivity did not disappear after 14 days in DM application proved the presence of T cells and showed that some of the T cells preserved their phenotypic properties. However, considering the biochemistry results, it was observed that the secretory capacity of the organoids increased at a higher proportion even when the Pt cell usage was minimal in the organoid establishment. These results indicated that Pt-like differentiation occurred. Even somehow phenotypic features of T cells were also preserved. Pt organoid was not showing PTH positivity in all cells according to the IHC results. Since PTH secretion is not always and Pt cells contain oxyphil cells in addition to chief cells, PTH positivity was not observed in all cells, despite the fact that Pt organoid was formed from only Pt cells. This was also true for COC samples, even if differentiation has occurred, PTH can be measured, but PTH staining may not be positive. Thus, IHC analysis results had to be considered with biochemistry results. Throughout the study, over 90 percent viability was observed in all organoid cultures. It has been stated in the literature that larger organoid sizes or longer incubation times may affect cell viability, and death is mostly observed in cells located in the center of spheroids, but according to our live/dead assay results, this type of cell death was not observed [98]. Dead cells were seen most particularly along the edges of the organoids. Loss of cell to cell contact and spheroid integration might be the reason behind of this localization of dead cells.

In order to determine the effects of differentiation medium application in terms of gene expression in organoids, cell specific gene expressions as PTH and CaSR were determined using qPCR method. While T organoid did not express PTH as expected, all COC organoids expressed PTH gene. When PTH expression results of COC organoids were compared with each other, the highest expression value was found in COC 1:1 (Pt:T) and the lowest expression value was observed in COC 1:16 (Pt:T). This result does not necessarily mean that higher percentage of Pt cells were required for higher PTH expression since the second highest PTH expression value belonged to COC 1:8 (Pt:T) rather than COC 1:2 (Pt:T). These results should be evaluated together with the results of biochemical analysis in order to make inferences on organoid functionality truly. When biochemistry and gene expression profile analysis results were evaluated together, it was observed that COC 1:1 (Pt:T) and COC 1:4 (Pt:T) groups showed the best Pt-like functionality among the other groups.

5. CONCLUSION

In the last decade, there has been a growing interest of generating 3D structures which resemble the functional and structural features of an organ *in vivo*. Although this revolutionary field has great potential in therapeutic medicine, it possesses still many hurdles as the organ to be mimicked is mostly superior *in vivo* and more complex with different cell types. The main strength of this study lies in the fact that Pt is the smallest organ in the human body and its functionality can only be achieved by chief cells. Therefore, Pt cells can be pioneers in organoid studies. This study was designed to create Pt-like structures by coculturing Pt and T cells due to its common origin in the embryological period and its close anatomical relationships in the adult period. We revealed that COC environment with Activin A and Shh included medium induced differentiation of stem cells found in T tissue into Pt-like cells. According to the biochemical and gene expression results, COC 1:1 (Pt:T) and COC 1:4 (Pt:T) groups showed the best Pt-like functionality among the other groups. This technique promises that organs of the same embryological origin may differentiate into desired cell type with the use of an appropriate differentiation medium. Furthermore, alternative solutions have been indirectly sought for the immune related and tissue compatibility problems encountered in allogenic Pt transplantations by increasing autogenically obtainable T cell amount in organoid formation. Thus, functional organoids created using fewer allogeneic cells have the potential to be transferred to the clinic without the need for immunosuppression in patients diagnosed with HypoPTH. This strategy to be followed, will not only provide a permanent treatment, but also will reduce the side effects and costs associated problems related to the use of immunosuppressors. Transplantation of COC organoids with Pt-like properties may be a potential solution to the problem of finding HLA-matched donors in patients awaiting organs.

6. FUTURE PROSPECTS

The aim of this study was to create functional Pt-like organoids from stem cells of T tissue in a COC environment including Shh and Activin A proteins. According to the results obtained in this study, the aim was achieved *in vitro.* However, longer-term (eg. 45 days) COC trials involving the same methods can be performed to strengthen the results. At specified time intervals, expression analysis of the T-specific marker can be performed in addition to the analyzed markers by qPCR. Furthermore, repeat of IHC analysis may provide a clearer result of the T-specific TTF1 analysis and thus T phenotype after DM treatment. In future studies, the results can be evaluated *in vivo* by implanting COC organoids in a model animal. In case of successful *in vivo* results, the next step should be transfer of the prepared organoids to the clinic by offering a potential therapeutic approach in the treatment of HypoPTH.

REFERENCES

1. Professor Owen FRS FZS &c. III. On the Anatomy of the Indian Rhinoceros (Rh. unicornis, L.). *Trans Zool Soc London*. 1852;4(2):31–58.

2. Johansson H. The Uppsala anatomist Ivar Sandström and the parathyroid gland. *Ups J Med Sci*. 2015;120(2):72–7.

3. Gley E. Sur la toxicité des urines des chiens thyroidectomisés: contribution à l'étude des fonctions du corps thyroide. *Comptes Rendus La Société Biol*. 1891;3:366–8.

4. MacCallum WG, Lambert RA, Vogel KM. The removal of calcium from the blood by dialysis in the study of tetany. *J Exp Med*. 1914;20(2):149–68.

5. Berkeley WN, Beebe SP. A contribution to the physiology and chemistry of the parathyroid gland. *J Med Res*. 1909;20(2):149.

6. von Eiselsberg A. Über erfolgreiche Einheilung der Katzenschilddrüse in die Bauchdecke und Auftreten von Tetanie nach deren Exstirpation 1892;(5), 81–85.

7. Collip JB. The extraction of a parathyroid hormone which will prevent or control parathyroid tetany and which regulates the level of blood calcium. *J Biol Chem*. 1925;63(2):395–438.

8. Rasmussen H, Craig LC. Purification of parathyroid hormone by use of countercurrent distribution. *J Am Chem Soc*. 1959;81(18):5003.

9. Norman AW, Henry HL. Calcium-Regulating Hormones:Vitamin D, Parathyroid Hormone, Calcitonin, and Fibroblast Growth Factor 23. *Hormones*.vol. 3. 2015th ed. 2015: 189–221.

10. Stewart WB, Rizzolo LJ. Embryology and Surgical Anatomy of the Thyroid and Parathyroid Glands BT - Surgery of the Thyroid and Parathyroid Glands. 2012: 15–23.

11. Akerström G, Malmaeus J, Bergström R. Surgical anatomy of human parathyroid glands. *Surgery*. 1984;95(1):14–21.

12. Oertli D, Udelsman R. Surgery of the thyroid and parathyroid glands. Berlin: Springer; 2007.

13. Arrangoiz R, Cordera F, Caba D, Juárez MM, Moreno E, Luque E. Parathyroid embryology, anatomy, and pathophysiology of primary hyperparathyroidism. *Int J Otolaryngol Head Neck Surg*. 2017;6(4):39–58.

14. Dream S. Parathyroidectomy. *Common Surgeries Made Easy A Quick Guid. Resid. Med. Students*. 2020: 261–5.

15. Frisdal A, Trainor PA. Development and evolution of the pharyngeal apparatus. *Wiley Interdiscip Rev Dev Biol*. 2014;3(6):403–18.

16. Hoang JK, Sung W, Bahl M, Phillips CD. How to perform parathyroid 4D CT: tips and traps for technique and interpretation. *Radiology*. 2014;270(1):15–24.

17. Phitayakorn R, McHenry CR. Incidence and location of ectopic abnormal parathyroid glands. *Am J Surg*. 2006;191(3):418–23.

18. Policeni BA, Smoker WRK, Reede DL. Anatomy and embryology of the thyroid and parathyroid glands. *Semin. Ultrasound, CT MRI*.vol. 33. 2012: 104–14.

19. Taterra D, Wong LM, Vikse J, Sanna B, Pękala P, Walocha J, et al. The prevalence and anatomy of parathyroid glands: a meta-analysis with implications for parathyroid surgery. *Langenbeck's Arch Surg*. 2019;404(1):63–70.

20. Baloch ZW, LiVolsi VA. Pathology of the parathyroid glands in hyperparathyroidism. *Semin. Diagn. Pathol.*vol. 30. 2013; 165–77.

21. Ranjan P. Applied bioinformatics for exploring diversity patterns in meta-omic data. Master Thesis, Georgia Institute of Technology, 2018.

22. Haschek WM, Rousseaux CG, Wallig MA. Chapter 17 - Endocrine System. 2010; 513–51.

23. Shi Y, Hogue J, Dixit D, Koh J, Olson JA. Functional and genetic studies of isolated cells from parathyroid tumors reveal the complex pathogenesis of parathyroid neoplasia. *Proc Natl Acad Sci USA*. 2014;111:3092-7.

24. Ritter CS, Haughey BH, Miller B, Brown AJ. Differential gene expression by oxyphil and chief cells of human parathyroid glands. *J Clin Endocrinol Metab*. 2012;97(8):E1499–505.

25. Wardle EN, Kurihara I, Saito T, Obara K, Shoji Y, Hirai M, et al. Oxyphil cell function in secondary parathyroid hyperplasia. *Nephron*. 1996;73(4):580–6.

26. Uhlén M, Fagerberg L, Hallström BM, Lindskog C, Oksvold P, Mardinoglu A, et al. Tissue-based map of the human proteome. *Science*. 2015;347(6220):1260419.

27. Munger BL, Roth SI. The cytology of the normal parathyroid glands of man and Virginia deer; a light and electron microscopic study with morphologic evidence of secretory activity. *J Cell Biol*. 1963;16(2):379–400.

28. Avilova O, Erokhina V. Ultramicroscopic changes in the parathyroid glands and thymus after immunostimulation in rats. *Arch Balk Med Union*. 2019;54(2):227–34.

29. Kumar V, Abbas AK, Aster JC. Robbins basic pathology e-book. 2017:

30. Rosol TJ, DeLellis RA, Harvey PW, Sutcliffe C. Chapter 58 - Endocrine System. 2013: 2391–492.

31. Goltzman D, Mannstadt M, Marcocci C. Physiology of the calcium-parathyroid hormone-vitamin D axis. *Vitam D Clin Med*. 2018;50:1–13.

32. Brown EM. Extracellular Ca2+ sensing, regulation of parathyroid cell function, and role of Ca2+ and other ions as extracellular (first) messengers. *Physiol Rev*. 1991;71(2):371–411.

33. Yu N, Donnan PT, Murphy MJ, Leese GP. Epidemiology of primary hyperparathyroidism in Tayside, Scotland, UK. *Clin Endocrinol (Oxf)*. 2009;71(4):485–93.

34. Yeh MW, Ituarte PHG, Zhou HC, Nishimoto S, Liu I-L, Harari A, et al. Incidence and prevalence of primary hyperparathyroidism in a racially mixed population. *J Clin Endocrinol Metab*. 2013;98(3):1122–9.

35. Clarke BL. Epidemiology of primary hyperparathyroidism. *J Clin Densitom*. 2013;16(1):8–13.

36. Marcocci C, Cetani F, Rubin MR, Silverberg SJ, Pinchera A, Bilezikian JP. Parathyroid carcinoma. *J Bone Miner Res*. 2008;23(12):1869–80.

37. Bilezikian JP, Bandeira L, Khan A, Cusano NE. Hyperparathyroidism. *Lancet*. 2018;391(10116):168–78.

38. Jamal SA, Miller PD. Secondary and tertiary hyperparathyroidism. *J Clin Densitom*. 2013;16(1):64–8.

39. Rothe HM, Liangos O, Biggar P, Petermann A, Ketteler M. Cinacalcet Treatment of Primary Hyperparathyroidism. *Int J Endocrinol*. 2011;2011:415719.

40. Clarke BL. Epidemiology and complications of hypoparathyroidism. *Endocrinol Metab Clin North Am*. 2018;47(4):771–82.

41. Poetzsch B, Smith JS. Hypoparathyroidism. *J Am Acad PAs*. 2012;25(1):60–2.

42. Marcucci G, Cianferotti L, Brandi ML. Clinical presentation and management of hypoparathyroidism. *Best Pract Res Clin Endocrinol Metab*. 2018;32(6):927–39.

43. Brandi ML, Bilezikian JP, Shoback D, Bouillon R, Clarke BL, Thakker R V, et al. Management of hypoparathyroidism: summary statement and guidelines. *J Clin Endocrinol Metab*. 2016;101(6):2273–83.

44. Sikjaer T, Rolighed L, Hess A, Fuglsang-Frederiksen A, Mosekilde L, Rejnmark L. Effects of PTH (1–84) therapy on muscle function and quality of life in hypoparathyroidism: results from a randomized controlled trial. *Osteoporos Int*. 2014;25(6):1717–26.

45. Watanabe A, Yoneyama S, Nakajima M, Sato N, Takao-Kawabata R, Isogai Y, et al. Osteosarcoma in Sprague-Dawley rats after long-term treatment with teriparatide (human parathyroid hormone (1-34)). *J Toxicol Sci*. 2012;37(3):617–29.

46. Hodsman AB, Bauer DC, Dempster DW, Dian L, Hanley DA, Harris ST, et al. Parathyroid Hormone and Teriparatide for the Treatment of Osteoporosis: A Review of the Evidence and Suggested Guidelines for Its Use. *Endocr Rev*. 2005;26(5):688–703.

47. Garcia-Roca R, Garcia-Aroz S, Tzvetanov IG, Giulianotti PC, Campara M, Oberholzer J, et al. Simultaneous living donor kidney and parathyroid allotransplantation: first case report and review of literature. *Transplantation.* 2016;100(6):1318–21.

48. Langer R, Vacanti JP. Tissue engineering. *Science*. 1993;260(5110):920–6.

49. Bergan A. Ancient myth, modern reality: a brief history of transplantation. *J Biocommun*. 1997;24(4):2–9.

50. Barker CF, Markmann JF. Historical overview of transplantation. *Cold Spring Harb Perspect Med*. 2013;3(4):a014977.

51. Dutkowski P, De Rougemont O, Clavien P. Alexis Carrel: genius, innovator and ideologist. *Am J Transplant*. 2008;8(10):1998–2003.

52. Lee H-S, Byun S-H, Cho S-W, Yang B-E. Past, Present, and Future of Regeneration Therapy in Oral and Periodontal Tissue: A Review. *Appl Sci*. 2019;9:1046.

53. Prodromos CC, Fu FH, Howell SM, Johnson DH, Lawhorn K. Controversies in soft-tissue anterior cruciate ligament reconstruction: grafts, bundles, tunnels, fixation, and harvest. *JAAOS-Journal Am Acad Orthop Surg*. 2008;16(7):376–84.

54. Bajaj P, Schweller RM, Khademhosseini A, West JL, Bashir R. 3D biofabrication strategies for tissue engineering and regenerative medicine. *Annu Rev Biomed Eng*. 2014;16:247–76.

55. Salgado AJ, Oliveira JM, Martins A, Teixeira FG, Silva NA, Neves NM, et al. Chapter One - Tissue Engineering and Regenerative Medicine: Past, Present, and Future. *Tissue Eng. Peripher. Nerve Stem Cells Regen. Promot. Factors*.vol. 108. 2013: 1–33.

56. Bingham EL, Cheng S-P, Woods Ignatoski KM, Doherty GM. Differentiation of human embryonic stem cells to a parathyroid-like phenotype. *Stem Cells Dev*. 2009;18(7):1071–80.

57. Ignatoski KMW, Bingham EL, Frome LK, Doherty GM. Differentiation of precursors into parathyroid-like cells for treatment of hypoparathyroidism. *Surgery*. 2010;148(6):1186–90.

58. Ignatoski KMW, Bingham EL, Frome LK, Doherty GM. Directed trans-differentiation of thymus cells into parathyroid-like cells without genetic manipulation. *Tissue Eng - Part C Methods*. 2011;17(11):1051–9.

59. Ryu K-H, Cho K-A, Park HS, Kim J-Y, Woo S-Y, Jo I, et al. Tonsil-derived mesenchymal stromal cells: evaluation of biologic, immunologic and genetic factors for successful banking. *Cytotherapy*. 2012;14(10):1193–202.

60. Park YS, Kim HS, Jin YM, Yu Y, Kim HY, Park HS, et al. Differentiated tonsil-derived mesenchymal stem cells embedded in Matrigel restore parathyroid cell functions in rats with parathyroidectomy. *Biomaterials*. 2015;65:140–52.

61. Merceron TK, Murphy S V. Chapter 14 - Hydrogels for 3D Bioprinting Applications. 2015: 249–70.

62. Park YS, Hwang JY, Jun Y, Jin YM, Kim G, Kim HY, et al. Scaffold-free parathyroid tissue engineering using tonsil-derived mesenchymal stem cells. *Acta Biomater*. 2016;35:215–27.

63. Jung SY, Kim HY, Oh HJ, Choi E, Cho MS, Kim HS. Feasibility of autologous plasma gel for tonsil-derived stem cell therapeutics in hypoparathyroidism. *Sci Rep*. 2018;8(1):1–8.

64. Lee CH, Wang YJ, Kuo SM, Chang SJ. Microencapsulation of parathyroid tissue with photosensitive poly (L-lysine) and short chain alginate-co-MPEG. *Artif Organs*. 2004;28(6):537–42.

65. Sethu P, Haglund TA, Rogers AJ, Chen H, Porterfield J, Balentine CJ. Growing Human Parathyroids in a Microphysiological System: A Novel Approach to Understanding and Developing New Treatments for Hyperparathyroidism. *Cells Tissues Organs*. 2019;206(1–2):54–61.

66. Zhang P, Zhang H, Dong W, Wang Z, Qin Y, Wu C, et al. Differentiation of Rat Adipose-Derived Stem Cells into Parathyroid-Like Cells. *Int J Endocrinol*.

2020;2020:1860842.

67. Kim EH, Kim SS, Kim JI, Cheon JM, Kim JH, Lee JC, et al. Differentiation of Human Adipose-Derived Stem Cells into Parathyroid Hormone-Secreting Cells 2020.

68. Lawton BR, Martineau C, Sosa JA, Roman S, Gibson CE, Levine MA, et al. Differentiation of parathyroid hormone expressing cells from human pluripotent stem cells. *Endocrinology*. 2020.

69. Raisz LG. Regulation by Calcium of Parathyroid Growth and Secretion in vitro. *Nature*. 1963;197(4872):1115–6.

70. Hamilton JW, Cohn D V. Studies on the Biosynthesis in Vitro of Parathyroid Hormone: I. Synthesis of parathyroid hormone by bovine parathyroid gland slices and its control by calcium. *J Biol Chem*. 1969;244(20):5421–9.

71. Capen CC. Fine structural alterations of parathyroid glands in response to experimental and spontaneous changes of calcium in extracellular fluids. *Am J Med*. 1971;50(5):598–611.

72. Brown EM, Hurwitz S, Aurbach GD. Preparation of Viable Isolated Bovine Parathyroid Cells. *Endocrinology*. 1976;99(6):1582–8.

73. Dietel M. By-pass secretion of human parathyroid adenomas. A particular intracellular form of rapid adaptation to external stimuli. 1980.

74. Björklund P, Hellman P. Culture of parathyroid cells. *Hum. Cell Cult. Protoc.* 2012; 43–53.

75. Liu W, Ridefelt P, Akerstrom G, Hellman P. Differentiation of human parathyroid cells in culture. *J Endocrinol*. 2001;168(3):417–26.

76. Roussanne M-C, Gogusev J, Hory B, Duchambon P, Souberbielle JC, Nabarra B, et al. Persistence of Ca2+-Sensing Receptor Expression in Functionally Active, Long-Term Human Parathyroid Cell Cultures. *J Bone Miner Res*. 1998;13(3):354–62.

77. Ridgeway RD, Hamilton JW, MacGregor RR. Characteristics of bovine parathyroid cell organoids in culture. *Vitr Cell Dev Biol*. 1986;22(2):91–9.

78. Sun F, Maercklein P, Fitzpatrick LA. Paracrine interactions among parathyroid cells: effect of cell density on cell secretion. *J Bone Miner Res*. 1994;9(7):971–6.

79. Huch M, Knoblich JA, Lutolf MP, Martinez-Arias A. The hope and the hype of organoid research. *Development*. 2017;144(6):938–41.

80. Park CS, Nguyen LP, Yong D. Development of Colonic Organoids Containing Enteric Nerves or Blood Vessels from Human Embryonic Stem Cells. *Cells* . 2020;9(10).

81. Treuting P.M., Dintzis S.M., Montine K.S. Endocrine System. *Comparative Anatomy and Histology*. 2018; 251–73.

82. Chen H, Senda T, Emura S, Kubo K. An update on the structure of the parathyroid gland. *Open Anat J*. 2013;5(1).

83. Wang Y, Li W, Phay JE, Shen R, Pellegata NS, Saji M, et al. Primary cell culture systems for human thyroid studies. *Thyroid*. 2016;26(8):1131–40.

84. Fong P. Chapter Two - Apical Iodide Efflux in Thyroid. *Horm. Transp. Syst.*vol. 98. 2015: 33–62.

85. Xiang L, Kong B. PAX8 is a novel marker for differentiating between various types of tumor, particularly ovarian epithelial carcinomas. *Oncol Lett*. 2013;5(3):735–8.

86. Vliet G Van. Development of the thyroid gland: lessons from congenitally hypothyroid mice and men. *Clin Genet*. 2003;63(6):445–55.

87. Cheng I, Klingensmith ME, Chattopadhyay N, Kifor O, Butters RR, Soybel DI, et al. Identification and localization of the extracellular calcium-sensing receptor in human breast. *J Clin Endocrinol Metab*. 1998;83(2):703–7.

88. Bisello A, Chorev M, Friedman PA, Gardella T, Hills R, Jueppner H, et al. Parathyroid hormone receptors (version 2019.4) in the IUPHAR/BPS Guide to Pharmacology Database. *IUPHAR/BPS Guid to Pharmacol CITE*. 2019;2019(4 SE-Summaries).

89. Cohn D, Fasciotto B, Reese B, Zhang J. Chromogranin A: a Novel Regulator of Parathyroid Gland Secretion. *J Nutr*. 1995;125:2015S-2019S.

90. Rix TE, Sinha P. Inadvertent parathyroid excision during thyroid surgery. *Surg*. 2006;4(6):339–42.

91. Rodríguez-Martínez G, Molina-Hernández A, Velasco I. Activin A Promotes Neuronal Differentiation of Cerebrocortical Neural Progenitor Cells. *PLoS One*. 2012;7(8):e43797.

92. Sulzbacher S, Schroeder IS, Truong TT, Wobus AM. Activin A-Induced Differentiation of Embryonic Stem Cells into Endoderm and Pancreatic Progenitors—The Influence of Differentiation Factors and Culture Conditions. *Stem Cell Rev Reports*. 2009;5(2):159–73.

93. Rowton M, Hoffmann AD, Steimle JD, Yang XH, Guzzetta A, Lazarevic S, et al. Hedgehog signaling controls progenitor differentiation timing during heart development. *BioRxiv*. 2018;270751.

94. Gomez-Fernandez C, Jorda M, Delgado PI, Ganjei-Azar P. Thyroid transcription factor 1. *Cancer Cytopathol*. 2002;96(5):289–93.

95. Dobrescu A, Cristi T, Cornianu M, Lazureanu C, Golu I, Tanasescu S, et al. Thyroid Transcription Factor - 1 (TTF-1) Immunoexpression in Thyroid Carcinoma with Follicular Origin. *Rev Chim*. 2020;71:185–91.

96. Erickson LA, Mete O. Immunohistochemistry in Diagnostic Parathyroid Pathology. *Endocr Pathol*. 2018;29(2):113–29.

97. Gogusev J, Murakami I, Telvi L, Goguin A, Sarfati E, Jaubert F. Establishment and characterization of a human parathyroid carcinoma derived cell line. *Pathol Res Pract*. 2015;211(4):332–40.

98. Ding B, Sun G, Liu S, Peng E, Wan M, Chen L, et al. Three-Dimensional Renal Organoids from Whole Kidney Cells: Generation, Optimization, and Potential Application in Nephrotoxicology In Vitro. *Cell Transplant*. 2020;29:963689719897066.